

Article

The Influence of Power Quality Indices on Active Power Losses in a Local Distribution Grid

Alena Otcenasova *, Andrej Bolf, Juraj Altus and Michal Regula

Department of Power Systems and Electric Drives, Faculty of Electrical Engineering and Information Technology, University of Zilina, Univerzitna 1, 010 26 Zilina, Slovakia; andrej.bolf@fel.uniza.sk (A.B.); juraj.altus@fel.uniza.sk (J.A.); michal.regula@fel.uniza.sk (M.R.)

* Correspondence: alena.otcenasova@fel.uniza.sk; Tel.: +421-41-513-2162

Received: 12 March 2019; Accepted: 9 April 2019; Published: 10 April 2019



Abstract: This paper deals with the topic of power quality in a local distribution grid. It is aimed to analyze the individual influences, which aggravate the power quality of the distribution grid. Based on the analysis, the most adverse effects were determined, and they were the voltage drops and supply voltage interruptions, supply voltage unbalance, load power factor, and also higher harmonics. These influences cause the technical losses in a distribution grid, which subsequently have a financial impact not only on the distribution, but also on the transmission of electricity. Only the load voltage unbalance, the load power factor, and the higher harmonics, which mainly cause the technical losses, were analyzed in this paper. The measurement of the influences of the adverse effects was performed on the model of a 22-kV distribution grid. The measurement was performed on the basis of three types of power line conductors and their different lengths, three types of active power consumption, and the different values of these adverse effects. According to this measurement, a simulation in program Matlab-Simulink was created. This simulation represented part of a 22-kV distribution grid, which was influenced by the abovementioned adverse effects. The results of the measurements were compared with the results of the simulation. Based on the evaluation of the technical losses from the measurement and the simulation, the financial losses during a certain period were calculated for the distribution system operators.

Keywords: power quality; voltage unbalance; power factor; harmonics; power losses

1. Introduction

The world is constantly affected by modernization. Increasing emphasis is being placed on reducing the consumption of mineral resources and on reducing the adverse effects (AEs) on the environment. In the field of power engineering, there are many issues related to reducing AEs on the environment, reducing the consumption of mineral resources, but also saving electrical energy. Greater emphasis is placed not only on generation, transmission, and consumption of electrical energy, but also on its quality. Electrical energy is the key commodity in modern society. It does not only power our laptops, televisions, radios, and other appliances, but it also provides us with many of the basic items for living and comfort, such as heating, cooling, and lighting, and of course it facilitates economic growth. In fact, it creates an immediate part of our life that many of us take for granted. The reality is that the widespread availability of this commodity and its reliability are the working result of one of humans' most complex creations. Man has built systems which consist of a large number of power-generating sources and power-consuming elements or loads interconnected through transmission and distribution lines, transformers, switching devices, and ancillary equipment [1–4]. These systems are expected to work around the clock transporting electrical energy in the desired

quality from the various locations where it is generated—power plants—to the locations where it is consumed—houses, factories, shopping malls, etc. Thus, it must be efficient and reliable [5].

Over the last years, we can see that the number of households are increasing, which means that more electrical energy is consumed. It is not only about traditional households, but electrical energy consumption is also increased in industry, where it is constantly being used to drive and operate various devices and machines [6]. Both electric utilities and end-users of electric power are becoming increasingly concerned about the quality of electric power [7].

The issue of power quality (PQ) in electrical systems is an increasing concern. Modern trends also come with a number of modern manufacturing technologies, and modern devices and appliances are their result, which creates higher demands on the PQ. The PQ is an umbrella concept for a multitude of individual types of power system disturbances. The term electrical PQ is generally used to assess and maintain the good quality of the power at the level of generation, transmission, distribution, and utilization of AC electrical power [8,9]. The PQ is influenced by many factors and its sustainability of parameters in the standard limits is often difficult. Its deterioration can be caused on the generation side and also on the transmission or consumption side. There are a number of reasons for the decrease in the AC supply system's quality, including natural ones such as lightning, flashover, equipment failure, faults, and forced ones, such as voltage distortions. A number of customers' equipment also pollute the supply system as they draw a non-sinusoidal current and behave as non-linear loads [9]. However, appliances with non-sinusoidal consumption or non-linear loads can have the most significant impact on the consumption measurement [10–12]. The non-linear loads generate harmonics, which leads to the distortion of the voltage and current waveforms and changes in the characteristics of supplied power [13]. The PQ is quantified in terms of voltage, current or frequency deviation of the supply system, which may result in failure or mal-operation of customers' equipment.

The PQ has become an important area of study in electrical engineering, especially in electric distribution and utilization systems. It has created a great challenge for both the electric utilities and the manufacturers. Utilities must supply consumers with good PQ for operating their equipment satisfactorily, and manufacturers must develop their electric equipment either to be immune to such disturbances or override them [9,14–16].

The problems of PQ are often related with power losses (PL) in electrical systems, mainly in distribution systems with voltage levels of 0.4 kV and 22 kV. These PL in distribution systems occur due to the presence of several technical factors. Power losses can be attributed to technical losses and non-technical losses. Technical PL directly depend on the network's characteristics and the mode of operation [17–19]. Based on the European Commission's policy and according to the European Commission's President Jose Manuel Barroso, an ambitious 40% greenhouse gas reduction target for 2030 was defined. An efficient electrical energy transmission can result in a PL reduction in electrical energy transmission through power lines, and is associated with the reduction of electrical energy generation, and subsequently, greenhouse gas emissions reduction [20]. Therefore, it is important to know and define the magnitude of the individual components of technical losses in consideration to the PQ in electrical energy transmission. Many studies are focused only on reducing the PL. The authors of different papers used different algorithms on the PL minimization. For example: glow-worm swarm optimization, particle swarm optimization, genetic algorithm, runner root algorithm, etc. Other authors have used FACTS devices or network reconfiguration on PL minimization [21–25]. We tried to find out the AEs that influenced the technical PL and determined their size in a local distribution grid. In low-voltage (LV) and medium-voltage (MV) networks, the voltage dip/swell and interruption, voltage unbalance, power factor of the fundamental frequency of electrical energy consumption (PF), and the higher harmonic orders were considered the most important AEs. Thanks to the present study, a part of the individual components of the technical PL in relation to the measured PQ in a local distribution grid can be determined. The study is also interesting for distribution system operators in relation to the financial costs reduction for covering the PL in electrical energy transmission.

2. Power Quality

Nowadays, PQ plays a very important role, as a large number of electronic devices in the Slovak Republic, and around the world, do not meet the quality parameters, which leads to problems with the PQ. End consumers are constantly worried about the deterioration of the PQ and also their electronic devices. The term “quality” is, in general, used to assess and maintain the good quality of power at the level of generation, transmission, and distribution, and on the other side, the use of electrical energy [26].

2.1. Voltage Unbalance

The voltage unbalance of the supply voltage is caused due to the uneven distribution of loads between the individual phases of the grid. It results in current unbalance, which causes the voltage unbalance in the grid. The standard [27] defines that 100% of the 10-minute average mean square value of the negative-phase sequence component of the supply voltage must be within the range of 0% to 2% of positive-phase sequence component during one week under normal operating conditions [15,28].

2.2. Voltage Deviation

The normalized phase voltage in a low-voltage distribution grid is 230 V. In the frame of standard operating conditions without interrupted periods, the voltage deviation should not exceed $\pm 10\%$ of the nominal voltage [15,27].

In cases of where the supply of electricity to the grids are not connected to a transmission system or to special remotely controlled users, voltage deviations cannot exceed $+10\%/ -15\%$ of the nominal voltage [15,27], and users must be informed about it.

2.3. Rapid Voltage Change

Rapid changes in the supply voltage are mainly due to changes in the load of grid users, grid switching or faults. Such changes shall be within the following limits at all supply terminals 100% of the time, as shown in Table 1 [15,27].

Table 1. Rapid voltage change [15].

Rapid Voltage Change	Max. Frequency for 24 h
$\Delta U_{\text{Steady state}} \geq 3\%$	24
$\Delta U_{\text{Max}} \geq 5\%$	24

2.4. Flicker Severity

Rapid supply voltage changes are mainly caused by changes in grid load, line switching, etc., and the flicker severity must be within the following limits, as shown in Table 2 [15,27].

Table 2. Parameters of flicker severity [15].

Flicker Severity	$0.23 \text{ kV} \leq U_n \leq 35 \text{ kV}$	Time Period	Measurement
Short-term severity P_{st} (pu)	1.2	95% of week	10 min
Long-term severity P_{lt} (pu)	1.0	100% of time	120 min

2.5. Power Factor of the Fundamental Frequency

The PF does not belong to the qualitative parameter and it has an influence on PL. The PF has been defined in several ways, and it can be said that PF is the ratio of working (active) power P to

apparent power S . It is also defined as the ratio of current drawn that produces real work to the total current drawn from the source or supplier of the energy, such as the electric utility [29].

$$\cos \varphi = \frac{P}{S} = \frac{P}{V \cdot I'} \quad (1)$$

where $\cos \varphi$ is the power factor of the fundamental frequency; P is active power; and S is the apparent power.

The distribution grids in MV transport energy to the distribution transformers, which feed predominantly inductive loads in most cases; this deteriorates the PF on a large scale, so it is necessary to implement compensation measures for the reactive power in these grids. These measures reduce the consumption of reactivities by minimizing the difference between the active and apparent powers, and thus improve the PF. Improving the PF implies a reduction of energy costs, release of the electrical capacity of the distribution system, and improvement of the voltage levels [30].

2.6. Harmonic and Interharmonic Voltage

The harmonic voltages (HCVs) represent voltages with sinusoidal waveform, whose frequency is an integer multiple of the fundamental frequency at which the supply system is designed to operate (50 Hz/60 Hz). If the frequency value of 50 Hz is considered as the fundamental frequency, then the third harmonic has a frequency of 150 Hz and the fifth harmonic 250 Hz. The cause of the occurrence of HCVs and currents are mainly non-linear loads, switching sources, arc furnace, semiconductor switching, etc. [15,28,31].

Total harmonic distortion (THD) of supply voltage shall not exceed 8% or 5% (LV, MV, HV level, respectively) as a mean value over 10 minutes of one week 100% of the time at all supply terminals [27]. The limits for individual harmonics of voltage for voltage level—low, medium, and high are defined in standard STN EN 50 160.

THD_V is determined as:

$$THD_V = \frac{\sqrt{\sum_{h=2}^{40} V_h^2}}{V_1} \times 100\% \leq 8\%, \quad (2)$$

where h is harmonic order, V_h is the size of the corresponding order harmonic, and V_1 is the size of the fundamental harmonic.

The interharmonic voltage (IHCV) means all of the sinusoidal voltages with a frequency that is not an integer multiple of the fundamental frequency 50 Hz. The cause of the occurrence of IHCV, currents are the same as in case of HCVs [15].

2.7. Voltage Dip, Overvoltage, and Supply Interruption

Generally, the voltage dips are caused by failures occurring in the installations of grid users or in the public distribution grid. Overvoltage is normally caused by switching operations and disconnecting loads. Both phenomena are unpredictable and mostly just random events. The annual occurrence varies depending on the type of power supply grid and the observation place [15].

The interruptions are naturally very unpredictable and vary depending on the place of occurrence and time. Nowadays, it is not possible to provide fully representative statistical results of interruption density measurements in all European grids [15].

2.8. Frequency of Power Supply

The Slovak Republic is synchronously interconnected with ENTSO-E (European Network of Transmission System Operators for Electricity) and so frequency of supply voltage must be 50 Hz [15]. Table 3 shows frequency values for normal operating conditions, which must be within the following ranges according to the standard [27]:

Table 3. Frequency of power supply in the Slovak Republic [15].

System	Mean Value of the Fundamental Frequency Measured over 10 s Intervals	Time
With the synchronous interconnection	50 Hz ± 0.1 Hz (49.5 Hz ... 50.5 Hz)	100% of the time
	50 Hz + 4%/−6% (47 Hz ... 52 Hz)	100% of the time
Without the synchronous connection	50 Hz ± 2% (49 Hz ... 51 Hz)	100% of the time
	50 Hz ± 15% (42.5 Hz ... 57.5 Hz)	100% of the time

3. Analysis of Power Losses in the Distribution Grid

This chapter is dedicated to the analysis of the PL of the electrical energy in the distribution grid for the voltage level of 22 kV that are caused by the transmission of electrical energy to the end consumers. The line loss rate is the main economic and technical indicator that comprehensively reflects the planning, design, production, operation, and management of the power grid [32]. Voltage drop and PL are caused by current flow during the electrical energy transmission from power plants to consumers via transmission and distribution lines. In the ideal case, the current is created only by the active component, which makes an appliance work and causes basic losses (BL). In addition to the active component, the magnitude of the current and also the BL can be increased by the other components, which do not active work, such as reactive current, current of harmonics or current unbalance.

3.1. Power Losses in Electric Network

The area of the PL analysis and calculation of the electrical energy is quite extensive and requires a different effort and difficulty for individual voltage levels. The larger the voltage of transmitted electrical energy, the easier the calculation and overall analysis. The PL in HV and extra-high voltage networks are determined by calculation using physical formulas. These formulas use the values from measurements of active power and voltage on individual network components and real network technical parameters. For the LV and the MV networks, another method of calculating the PL is used [33]. The total electrical energy losses (ΔW) can be determined as the difference between the electrical energies entering to the network (W_I) and the electrical energies consumed by customers (W_O) and the electrical energy of self-consumption (W_V). The unit of ΔW is kWh.

$$\Delta W = \sum_1^k W_I - \left(\sum_1^k W_O + \sum_1^k W_V \right). \tag{3}$$

To show the total electric network losses, and to make losses easier to investigate, it is necessary to classify the network losses into different types, as indicated in Figure 1.

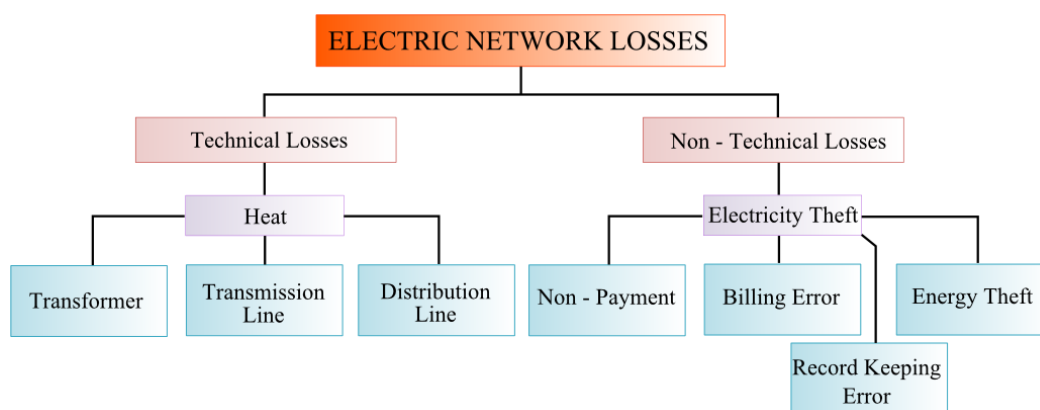


Figure 1. Power losses qualification in electric network.

Distribution PL can be divided into two categories: technical and non-technical losses, as is shown in Figure 1 [34]. The term technical losses mean that the losses are caused by transformation and transmission of electrical energy. For example, it is the electrical energy that is transformed into heat by passing through transformers, overhead lines, and other devices. Further, they are caused by well-known physical electricity effects such as harmonics distortion, long single-phase line, unbalanced loading, losses due to the effect of overloading and low voltage, etc. It depends on the network's properties and its mode of operation [35,36]. The technical losses can be divided into two classes [37]:

- Fixed Technical Losses—represent between 1/4–1/3 of total technical losses in a distribution network. These are usually in the form of heat and noise and can occur whenever the transformer is energized. The fixed losses are not influenced by the amount of load current flowing, but rather by corona losses, dielectric losses, leakage current losses, etc.
- Variable Technical Losses—are proportional to the square of the load current and accounts for between 2/3 and 3/4 of the technical losses in a distribution system. The variable losses arise due to the effects of line impedance, contact resistance, and joule heating losses.

Non-technical losses, also called commercial losses, sometimes creates a bigger share of total losses than the technical losses in LV networks. They are caused by actions external to the power system or by load conditions [38]. These losses are more difficult to measure, because they are often unaccounted for by system operators, and thus have no records. They can be determined as the difference between the total losses and calculated technical losses [39]. The most probable causes of non-technical losses are electricity theft, non-payment of bills by customers, errors in technical losses computation, and errors in accounting and record keeping that distort technical information as indicated in Figure 1.

In the Slovak Republic, the methodology used for the identification and distribution of technical losses was determined by the Decree of the Ministry of Industry and Trade of the Czech Republic. This decree is no longer valid, but still continues to be used, because no repeal has been issued for this decree.

3.2. Calculation of Electrical Losses in a Medium-Voltage Grids without Considering the Mutual Inductance

Electrical losses are caused by the current flowing through individual overhead lines due to their electrical parameters. Some parts of losses are converted into heat—called Joule losses—and other parts of losses are called magnetic field losses. Total PL ΔS can be defined as:

$$\sum_{k=1}^n \Delta S = \sum_{k=1}^n S_s - \sum_{k=1}^n S_e, \quad (4)$$

where S_s is the apparent power at the start of the power line; S_e is the apparent power at the end of the power line.

We can say that the total PL are a difference between the produced power of generators and the consumed power of loads. For one phase of the power line, if we do not dismiss the mutual inductance, the total PL can be defined by the Formula (4):

$$\begin{aligned} \Delta S_1 &= S_{1s} - S_{1e} = V_{1s} \cdot I_1^* - V_{1e} \cdot I_1^* = (V_{1s} - V_{1e}) \cdot I_1^* \\ &= (V_{1s} - (V_{1s} - \Delta V_1)) \cdot I_1^* = \Delta V_1 \cdot I_1^* = Z_1 \cdot I_1 \cdot I_1^* = ((R_1 + jX_{L1}) \cdot I_1) \cdot I_1^* \\ &= (R_1 + jX_{L1}) \cdot I_1^2 = R_1 \cdot I_1^2 + jX_{L1} \cdot I_1^2 = \Delta P_1 + j\Delta Q_1, \end{aligned} \quad (5)$$

where S_{1s} is the apparent power at the start of the power line; S_{1e} is the apparent power at the end of the power line; V_{1s} is the voltage at the start of the one phase of the power line; V_{1e} is the voltage at the end of the one phase of the power line; I_1^* is the conjugate complex current of the one phase of the power line; I_1 is the current of the one phase of the power line.

The result from Formula (5) is that the total PLs were calculated only as the sum of active and reactive power losses on the power line.

The active power losses (APLs) ΔP_1 can be defined according to Formula (5) as [40]:

$$\Delta P_1 = R_1 \cdot I_1^2 = R_1 \cdot (I_{1A}^2 + I_{1R}^2) = \frac{R_1}{V^2} \cdot (P^2 + Q^2), \quad (6)$$

where I_{1A} is the active component of the current; I_{1R} is the reactive component of the current.

From Formula (6) it follows that the APL depends on an active and a reactive component of the current flowing through the resistance of the power line R [41]. Increases in the APL are caused by the reactive component of the current. For this reason, this reactive component of the current has to be minimized by compensation and then the APL on the line will be the smallest.

The reactive power losses (RPLs) ΔQ_1 can be defined according to Formula (5):

$$\Delta Q_1 = X_{L11} \cdot I_1^2 = X_{L11} \cdot (I_{1A}^2 + I_{1R}^2) = \frac{X_{L11}}{V^2} \cdot (P^2 + Q^2), \quad (7)$$

where X_{L11} is the self-inductance of the power line.

From Formula (7) it follows, that the RPL depends on the current flowing through the inductive reactance of power line X_L and also from active and reactive component of this current.

The total APL and RPL in percent $\Delta P\%$, $\Delta Q\%$ are:

$$\begin{aligned} \Delta P\% &= \frac{\Delta P}{P_{\text{start}}} \times 100 = \frac{P_{\text{start}} - P_{\text{end}}}{P_{\text{start}}} \times 100, \\ \Delta Q\% &= \frac{\Delta Q}{Q_{\text{start}}} \times 100 = \frac{Q_{\text{start}} - Q_{\text{end}}}{Q_{\text{start}}} \times 100, \end{aligned} \quad (8)$$

where P_{start} and Q_{start} are the active power and reactive power at the start of the power line; P_{end} and Q_{end} are the active power and reactive power at the end of the power line.

3.3. Calculation of Losses in a Medium-Voltage Grid Considering the Mutual Inductance

The total PL ΔS considering the mutual inductance for one phase of the power line with a length of 1 km can be defined as:

$$\begin{aligned} \Delta S_1 &= S_{1s} - S_{1e} = V_{1s} \cdot I_1^* - V_{1e} \cdot I_1^* = (V_{1s} - V_{1e}) \cdot I_1^* \\ &= (V_{1s} - (V_{1s} - \Delta V_1)) \cdot I_1^* = \Delta V_1 \cdot I_1^* = (\Delta V_{R1} + \Delta V_{L1}) \cdot I_1^*. \end{aligned} \quad (9)$$

If the line drop is appointed to Formula (9), then:

$$\begin{aligned} \Delta S_1 &= (\Delta V_{R1} + \Delta V_{L11} + \Delta V_{L12} + \Delta V_{L13}) \cdot I_1^* \\ &= (R_1 \cdot I_1 + jX_{L11} \cdot I_1 + jX_{L12} \cdot I_2 + jX_{L13} \cdot I_3) \cdot I_1^* \\ &= R_1 \cdot I_1 \cdot I_1^* + j \cdot (X_{L11} \cdot I_1 + X_{L12} \cdot I_2 + X_{L13} \cdot I_3) \cdot I_1^* \\ &= R_1 \cdot I_1 \cdot I_1^* + j \cdot (X_{L11} \cdot I_1 \cdot I_1^* + X_{L12} \cdot I_2 \cdot I_1^* + X_{L13} \cdot I_3 \cdot I_1^*), \end{aligned} \quad (10)$$

where ΔV_{R1} is the voltage drop on the resistance of the power line; ΔV_{L1} is the voltage drop on the inductance of the power line; ΔV_{L11} is the voltage drop on the self-inductance of the power line; ΔV_{L12} and ΔV_{L13} are the voltage drops on the mutual inductance of the power line.

If the phasors in Formula (10) are overwritten using the goniometric functions:

$$\begin{aligned} \Delta S_1 &= R_1 \cdot I_1^2 \cdot (\cos \varphi_{11} - j \sin \varphi_{11}) \cdot (\cos \varphi_{11} + j \sin \varphi_{11}) \\ &+ j \cdot \left(\begin{aligned} &X_{L11} \cdot I_1^2 \cdot (\cos \varphi_{11} - j \sin \varphi_{11}) \cdot (\cos \varphi_{11} + j \sin \varphi_{11}) \\ &+ X_{L12} \cdot I_1 \cdot I_2 \cdot (\cos \varphi_{11} - j \sin \varphi_{11}) \cdot (\cos \varphi_{12} + j \sin \varphi_{12}) \\ &+ X_{L13} \cdot I_1 \cdot I_3 \cdot (\cos \varphi_{11} - j \sin \varphi_{11}) \cdot (\cos \varphi_{13} + j \sin \varphi_{13}) \end{aligned} \right), \end{aligned} \quad (11)$$

where I_1 is the own current flowing through the conductor; I_2 and I_3 are currents flowing through the other conductors; φ_{11} , φ_{12} , and φ_{13} are the angles between the current and real axis.

If the round brackets of the goniometric functions in Formula (11) are multiplied:

$$\Delta S_1 = R_1 \cdot I_1^2 \cdot \left(\begin{array}{l} \cos \varphi_{11} \cdot \cos \varphi_{11} + \sin \varphi_{11} \cdot \sin \varphi_{11} \\ + j \cdot (\cos \varphi_{11} \cdot \sin \varphi_{11} - \sin \varphi_{11} \cdot \cos \varphi_{11}) \end{array} \right) + j \cdot \left(\begin{array}{l} X_{L11} \cdot I_1^2 \cdot \left(\begin{array}{l} \cos \varphi_{11} \cdot \cos \varphi_{11} + \sin \varphi_{11} \cdot \sin \varphi_{11} \\ + j \cdot (\cos \varphi_{11} \cdot \sin \varphi_{11} - \sin \varphi_{11} \cdot \cos \varphi_{11}) \end{array} \right) \\ + X_{L12} \cdot I_1 \cdot I_2 \cdot \left(\begin{array}{l} \cos \varphi_{11} \cdot \cos \varphi_{12} + \sin \varphi_{11} \cdot \sin \varphi_{12} \\ + j \cdot (\cos \varphi_{11} \cdot \sin \varphi_{12} - \sin \varphi_{11} \cdot \cos \varphi_{12}) \end{array} \right) \\ + X_{L13} \cdot I_1 \cdot I_3 \cdot \left(\begin{array}{l} \cos \varphi_{11} \cdot \cos \varphi_{13} + \sin \varphi_{11} \cdot \sin \varphi_{13} \\ + j \cdot (\cos \varphi_{11} \cdot \sin \varphi_{13} - \sin \varphi_{11} \cdot \cos \varphi_{13}) \end{array} \right) \end{array} \right) \quad (12)$$

The following formula applies to the goniometric functions:

$$\begin{aligned} \cos(x) \cdot \cos(x) + \sin(x) \cdot \sin(x) &= 1, \\ \cos(x) \cdot \sin(x) - \sin(x) \cdot \cos(x) &= 0, \\ \cos(x) \cdot \cos(y) + \sin(x) \cdot \sin(y) &= \cos(x - y), \\ \cos(x) \cdot \sin(y) - \sin(x) \cdot \cos(y) &= -\sin(x - y), \end{aligned} \quad (13)$$

after applying Formula (13), we can modify Formula (12) as follows:

$$\Delta S_1 = R_1 \cdot I_1^2 + jX_{L11} \cdot I_1^2 + jX_{L12} \cdot I_1 \cdot I_2 \cdot (\cos \varphi_{112} - j \sin \varphi_{112}) + jX_{L13} \cdot I_1 \cdot I_3 \cdot (\cos \varphi_{113} - j \sin \varphi_{113}), \quad (14)$$

where $\varphi_{112} = \varphi_{11} - \varphi_{12}$ is the difference of the current angle of I_1 and I_2 ; $\varphi_{113} = \varphi_{11} - \varphi_{13}$ is the difference of the current angles of I_1 and I_3 .

After the next modification of Formula (14):

$$\begin{aligned} \Delta S_1 &= R_1 \cdot I_1^2 + jX_{L11} \cdot I_1^2 + jX_{L12} \cdot I_1 \cdot I_2 \cdot \cos \varphi_{112} \\ &+ X_{L12} \cdot I_1 \cdot I_2 \cdot \sin \varphi_{112} + jX_{L13} \cdot I_1 \cdot I_3 \cdot \cos \varphi_{113} + X_{L13} \cdot I_1 \cdot I_3 \cdot \sin \varphi_{113} \\ &= I_1 \cdot (R_1 \cdot I_1 + X_{L12} \cdot I_2 \cdot \sin \varphi_{112} + X_{L13} \cdot I_3 \cdot \sin \varphi_{113}) \\ &+ j \cdot (X_{L11} \cdot I_1 + X_{L12} \cdot I_2 \cdot \cos \varphi_{112} + X_{L13} \cdot I_3 \cdot \cos \varphi_{113}) \cdot I_1 = \cdot P_1 + j \cdot Q_1. \end{aligned} \quad (15)$$

From Formula (15) above, it follows that the total PL ΔS_1 of the first conductor of the three-phase system equals to the sum of APL and RPL on the power line. The total PL for the other power line conductors, ΔS_1 and ΔS_2 , will be calculated analogously to the respect of the inferior index:

$$\begin{aligned} \Delta S_2 &= jX_{L21} \cdot I_1 \cdot I_2 \cdot \cos \varphi_{121} + R_2 \cdot I_2^2 + jX_{L22} \cdot I_2^2 \\ &+ X_{L21} \cdot I_1 \cdot I_2 \cdot \sin \varphi_{121} + jX_{L23} \cdot I_2 \cdot I_3 \cdot \cos \varphi_{123} + X_{L23} \cdot I_2 \cdot I_3 \cdot \sin \varphi_{123} \\ &= I_2 \cdot (X_{L21} \cdot I_1 \cdot \sin \varphi_{121} + R_2 \cdot I_2 + X_{L23} \cdot I_3 \cdot \sin \varphi_{123}) \\ &+ j \cdot (X_{L21} \cdot I_1 \cdot \cos \varphi_{121} + X_{L22} \cdot I_2 + X_{L23} \cdot I_3 \cdot \cos \varphi_{123}) \cdot I_2, \\ \Delta S_3 &= jX_{L31} \cdot I_1 \cdot I_3 \cdot \cos \varphi_{131} + jX_{L33} \cdot I_3^2 + R_3 \cdot I_3^2 \\ &+ X_{L31} \cdot I_1 \cdot I_3 \cdot \sin \varphi_{131} + jX_{L32} \cdot I_2 \cdot I_3 \cdot \cos \varphi_{132} + X_{L32} \cdot I_2 \cdot I_3 \cdot \sin \varphi_{132} \\ &= I_3 \cdot (X_{L31} \cdot I_1 \cdot \sin \varphi_{131} + X_{L32} \cdot I_2 \cdot \sin \varphi_{132} + R_3 \cdot I_3) \\ &+ j \cdot (X_{L31} \cdot I_1 \cdot \cos \varphi_{131} + X_{L32} \cdot I_2 \cdot \cos \varphi_{132} + X_{L33} \cdot I_3) \cdot I_3. \end{aligned} \quad (16)$$

The APL for the individual conductors of a MV power line will be defined with Formula (16) as:

$$\begin{aligned} \Delta P_1 &= R_1 \cdot I_1^2 + X_{L12} \cdot I_1 \cdot I_2 \cdot \sin \varphi_{112} + X_{L13} \cdot I_1 \cdot I_3 \cdot \sin \varphi_{113}, \\ \Delta P_2 &= R_2 \cdot I_2^2 + X_{L21} \cdot I_1 \cdot I_2 \cdot \sin \varphi_{121} + X_{L23} \cdot I_2 \cdot I_3 \cdot \sin \varphi_{123}, \\ \Delta P_3 &= R_3 \cdot I_3^2 + X_{L31} \cdot I_1 \cdot I_3 \cdot \sin \varphi_{131} + X_{L32} \cdot I_2 \cdot I_3 \cdot \sin \varphi_{132}, \end{aligned} \quad (17)$$

and the RPL can be defined as:

$$\begin{aligned}\Delta Q_1 &= X_{L11} \cdot I_1^2 + X_{L12} \cdot I_1 \cdot I_2 \cdot \cos \varphi_{112} + X_{L13} \cdot I_1 \cdot I_3 \cdot \cos \varphi_{113}, \\ \Delta Q_2 &= X_{L22} \cdot I_2^2 + X_{L21} \cdot I_1 \cdot I_2 \cdot \cos \varphi_{121} + X_{L23} \cdot I_2 \cdot I_3 \cdot \cos \varphi_{123}, \\ \Delta Q_3 &= X_{L33} \cdot I_3^2 + X_{L31} \cdot I_1 \cdot I_3 \cdot \cos \varphi_{131} + X_{L32} \cdot I_2 \cdot I_3 \cdot \cos \varphi_{132}.\end{aligned}\quad (18)$$

As can be seen from Formula (17), the APL for the individual conductors of power lines depends not only on their resistances, but also on the mutual inductive reactances. The APL are primarily created by the current flowing through the resistances of the power line. These losses are also increased by the currents flowing through the other conductors, on the basis of their mutual inductances. Their magnitude depends on the magnitude of the currents flowing through the other conductors and on the sinus of the angle difference between its own current and the currents flowing through the other conductors.

The RPL for the individual conductors of the power lines mainly depends on its own inductive reactance. These losses are also increased by the currents flowing through the other conductors due to their mutual inductive reactances. Their magnitude depends on the magnitude of its own current, the magnitude of the currents flowing through the other conductors, and the cosinus of the angle difference between its own current and the currents flowing through the other conductors.

The total APL and RPL of the individual conductors of the power line and the complete system can be calculated as the difference of the active and the reactive powers at the start of the power line and at the end of the power line.

The total PL of the all three-phase system can be defined as:

$$\Delta S_C = \Delta S_1 + \Delta S_2 + \Delta S_3. \quad (19)$$

If Formulas (15) and (16) are appointed to Formula (19):

$$\begin{aligned}\Delta S_C &= R_1 \cdot I_1^2 + R_2 \cdot I_2^2 + R_3 \cdot I_3^2 \\ &+ X_{L12} \cdot I_1 \cdot I_2 \cdot \sin \varphi_{112} + X_{L13} \cdot I_1 \cdot I_3 \cdot \sin \varphi_{113} \\ &+ X_{L21} \cdot I_1 \cdot I_2 \cdot \sin \varphi_{121} + X_{L23} \cdot I_2 \cdot I_3 \cdot \sin \varphi_{123} \\ &+ X_{L31} \cdot I_1 \cdot I_3 \cdot \sin \varphi_{131} + X_{L32} \cdot I_2 \cdot I_3 \cdot \sin \varphi_{132}\end{aligned}\quad (20)$$

$$+ j \cdot \left(\begin{array}{l} X_{L11} \cdot I_1^2 + X_{L22} \cdot I_2^2 + X_{L33} \cdot I_3^2 \\ + X_{L12} \cdot I_1 \cdot I_2 \cdot \cos \varphi_{112} + X_{L13} \cdot I_1 \cdot I_3 \cdot \cos \varphi_{113} \\ + X_{L21} \cdot I_1 \cdot I_2 \cdot \cos \varphi_{121} + X_{L23} \cdot I_2 \cdot I_3 \cdot \cos \varphi_{123} \\ + X_{L31} \cdot I_1 \cdot I_3 \cdot \cos \varphi_{131} + X_{L32} \cdot I_2 \cdot I_3 \cdot \cos \varphi_{132} \end{array} \right)$$

and if the condition below is valid:

$$X_{12} = X_{21}, X_{13} = X_{31}, X_{23} = X_{32}, \quad (21)$$

then Formula (20) can be modified as:

$$\begin{aligned}\Delta S_C &= R_1 \cdot I_1^2 + R_2 \cdot I_2^2 + R_3 \cdot I_3^2 \\ &+ X_{L12} \cdot I_1 \cdot I_2 \cdot (\sin \varphi_{112} + \sin \varphi_{121}) + X_{L13} \cdot I_1 \cdot I_3 \cdot (\sin \varphi_{113} + \sin \varphi_{131}) \\ &+ X_{L23} \cdot I_2 \cdot I_3 \cdot (\sin \varphi_{123} + \sin \varphi_{132})\end{aligned}\quad (22)$$

$$+ j \cdot \left(\begin{array}{l} X_{L11} \cdot I_1^2 + X_{L22} \cdot I_2^2 + X_{L33} \cdot I_3^2 \\ + X_{L12} \cdot I_1 \cdot I_2 \cdot (\cos \varphi_{112} + \cos \varphi_{121}) \\ + X_{L13} \cdot I_1 \cdot I_3 \cdot (\cos \varphi_{113} + \cos \varphi_{131}) \\ + X_{L23} \cdot I_2 \cdot I_3 \cdot (\cos \varphi_{123} + \cos \varphi_{132}) \end{array} \right)$$

If the following formulas of goniometric functions are applied:

$$\begin{aligned}\sin(x - y) + \sin(y - x) &= 0, \\ \cos(x - y) + \cos(y - x) &= 2 \cdot \cos(y - x),\end{aligned}\quad (23)$$

Formula (22) can be reduced to:

$$\Delta S_C = R_1 \cdot I_1^2 + R_2 \cdot I_2^2 + R_3 \cdot I_3^2 + j \cdot \left(\begin{array}{l} X_{L11} \cdot I_1^2 + X_{L22} \cdot I_2^2 + X_{L33} \cdot I_3^2 \\ + X_{L12} \cdot I_1 \cdot I_2 \cdot 2 \cdot \cos \varphi_{112} \\ + X_{L13} \cdot I_1 \cdot I_3 \cdot 2 \cdot \cos \varphi_{113} \\ + X_{L23} \cdot I_2 \cdot I_3 \cdot 2 \cdot \cos \varphi_{123} \end{array} \right) = \Delta P_C + j \Delta Q_C. \quad (24)$$

Formula (24) represents the total PL of the MV three-phase system. Based on previous formula, it can be said that the inductive reactance of the power line contributes to the total PL in an MV grid, but does not participate in the APL. The losses can be influenced by the type of the conductor and the arrangement of conductors on the console, but also by changing the frequency.

According to Formula (24), the PL can be divided to the APL and RPL. For the total APL of an MV three-phase system grid apply:

$$\Delta P_C = \Delta P_1 + \Delta P_2 + \Delta P_3 = R_1 \cdot I_1^2 + R_2 \cdot I_2^2 + R_3 \cdot I_3^2. \quad (25)$$

Based on Formula (25), it can be said that the total APL depends only on the currents flowing through the resistance of the individual power line conductors. In comparison to Formula (17), the total APL of one power line conductor depends on the mutual inductances. It is caused by power flow between the individual conductors of the power line.

From Formula (25) and from the other previous formulas, the magnitude of the APL depends on:

- the magnitude of the individual conductors' resistance R ,
- the magnitude of the current flowing through the individual power line conductors—the load unbalance,
- the current magnitude of the active and the reactive component—the PF,
- the magnitude of root mean square value of the current and its frequency—the higher harmonic orders.

4. Analysis of Quality Parameters' Influence on the Power Losses in a Distribution Grid

The greatest noticeable value for the distribution system operators is the losses of active energy—the APL. The total APL, as it was mentioned before, consists of the BLs that were created by the transmission of the active power and from the additional losses caused by the transmission of reactive power, distortion power, and power imbalance. The simple simulation model and script were created due to the results of all figures in this chapter. This model helped us to determine the size of APL from the three-phase active power consumption for different types and lengths of power line conductors. In the simulation, the size of the APL was calculated by the active power at the start of power line minus the active power at the end of power line. It means that the difference was between the active power injected into the power line and the active power consumption.

4.1. Basic Active Power Losses

The basic APLs are the losses exist in every electric network, regardless of the occurrence of adverse effects. However, their magnitude depends on the voltage level of the distribution grid, and the type and length of the conductors and transformers that are used. These basic losses are increased by AEs such as load unbalance, PF, and the higher harmonic orders.

For a better overview of basic APLs, the graphic dependencies are shown in the following Figures 2–4. The graphs show the dependence between the three-phase active power consumption P_{abc} and the APL

ΔP for different types and lengths of aluminium conductor steel reinforced—ACSR—conductors. Three types of ACSR conductor were used ACSR 42/7, ACSR 70/11, and ACSR 95/15. The first number behind ACSR means the cross-section of aluminium and the second number is the cross-section of steel.

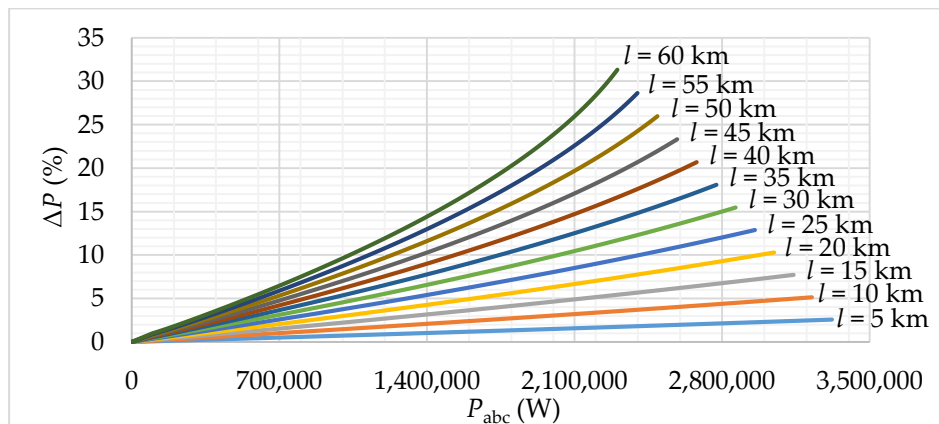


Figure 2. The dependence of increasing active power losses (APL) from three-phase active power consumption for aluminium conductor steel reinforced (ACSR) 42/7 without consideration of voltage dip.

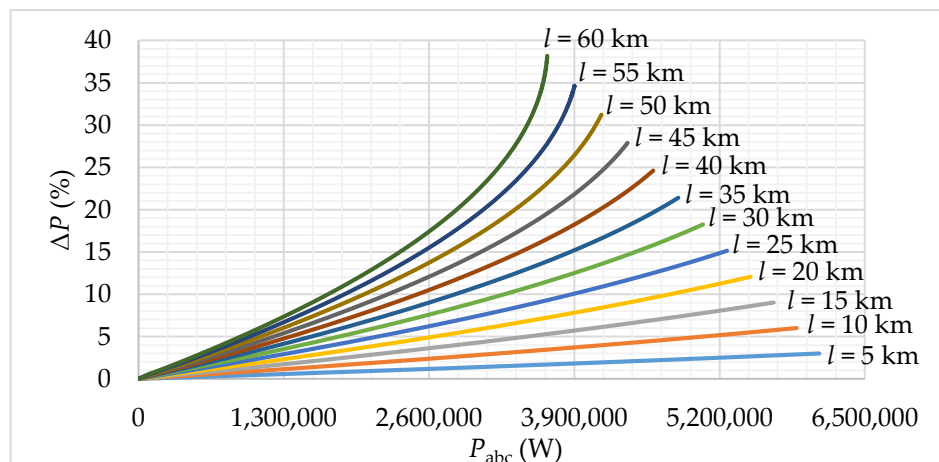


Figure 3. The dependence of increasing APL from three-phase active power consumption for ACSR 70/11 without consideration of voltage dip.

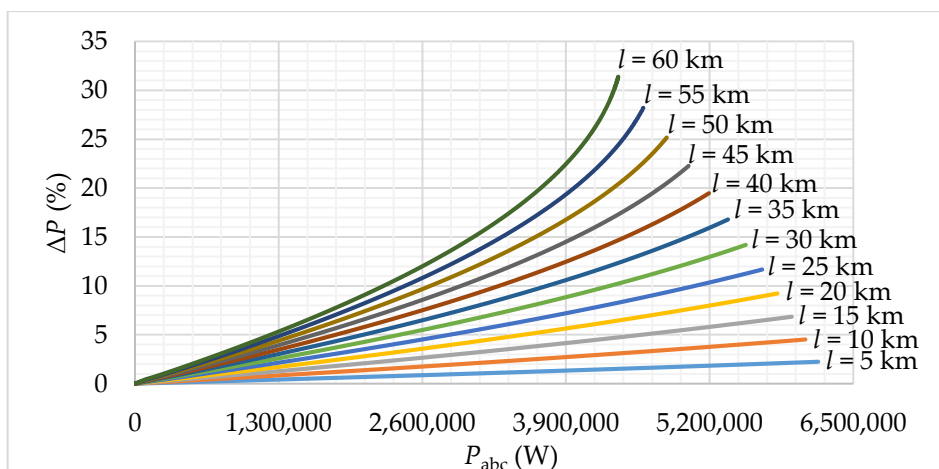


Figure 4. The dependence of increasing APLs from three-phase active power consumption for ACSR 95/15 without consideration of voltage dip.

From these graphs, it can be seen that if the three-phase active power consumption increased, then the APLs on the power line also increased. In addition, if the length of the power line is longer, then the APLs for the corresponding three-phase active power consumption are also larger. Maximal value of APLs and three-phase active power consumption is limited by the current loading capacity of the individual type of conductor. This current loading capacity is different for every conductor. For conductor ACSR 42/7 it is 153 A, for ACSR 70/11 it is 290 A, and for ACSR 95/15 it is 350 A. These values of current loading capacity are table values. However, the conductors are loaded for about 30% in real operation. In this study, the value of 60% of the current loading capacity was used. If the conductor's cross-section was bigger, its current loading capacity would be bigger, and the losses would be lower in comparison with the thinner conductor. This is the case when the maximal value of APLs and three-phase active power consumption is limited by the power line current loading capacity and also when the voltage value is limited by $12.7 \text{ kV} \pm 10\%$ (according to the standard STN EN 50160) at the end of the power line to avoid a voltage dip, as shown in Figures 5–7.

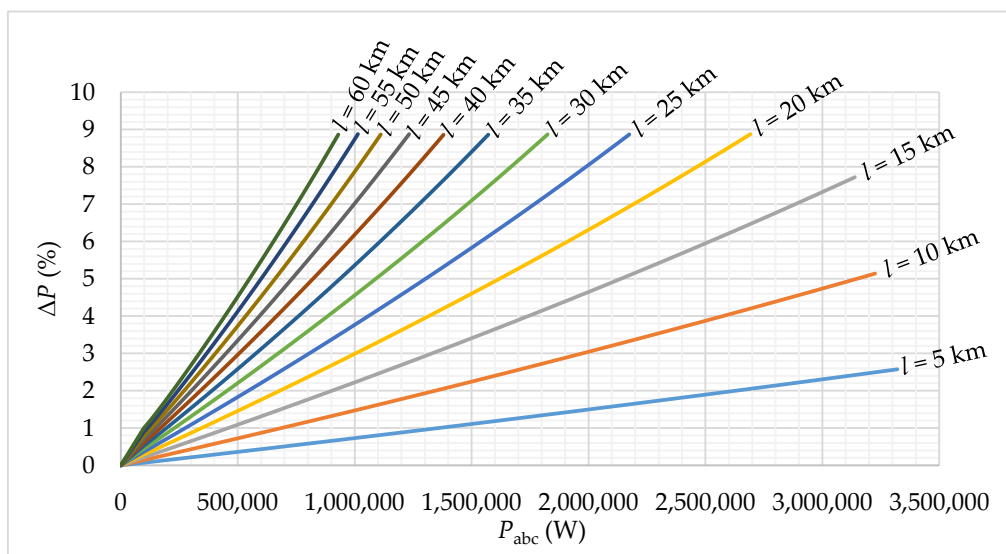


Figure 5. The dependence of increasing APLs from three-phase active power consumption for ACSR 42/7 with consideration of voltage dip.

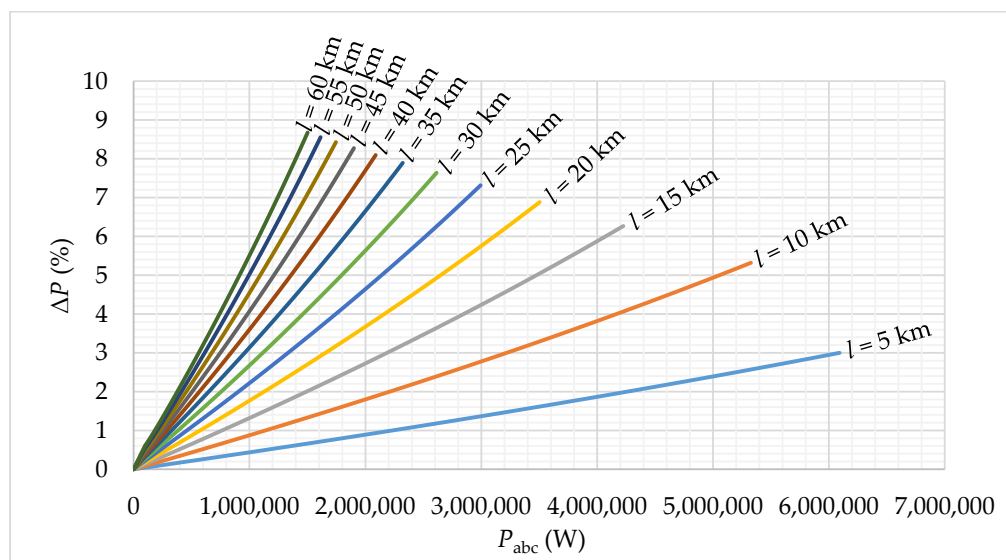


Figure 6. The dependence of increasing APLs from three-phase active power consumption for ACSR 70/11 with consideration of voltage dip.

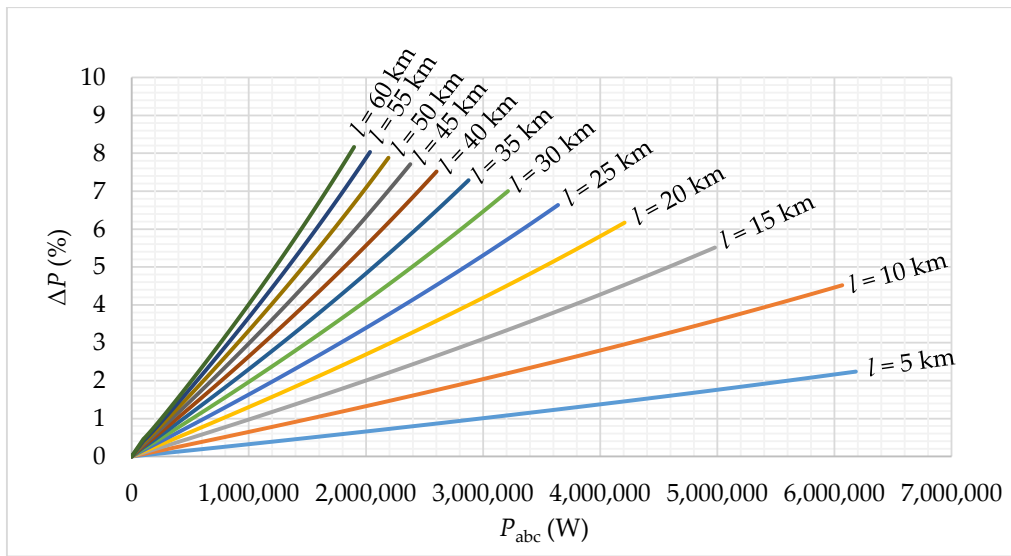


Figure 7. The dependence of increasing APLs from three-phase active power consumption for ACSR 95/15 with consideration of voltage dip.

4.2. The Influence of Load Unbalance on Active Power Losses

The magnitude of the total APLs was influenced by load unbalance more than power line unbalance. The load unbalance caused the different current flows in the power line and the different line voltages to drop. Every state of load unbalance caused an increase of the total APLs in the grid compared to the symmetrical state. Five scenarios were examined to show the increase of total APLs:

- **Scenario 1:** the load change of phases A, B, and C (equally)—the symmetrical state,
- **Scenario 2:** the load change of phase A, phase B = phase C = 0,
- **Scenario 3:** the load change of phases A and B (equally), phase C = 0,
- **Scenario 4:** the load change of phase B, phase A = max., phase C = 0,
- **Scenario 5:** the load change of phases B and C (equally), phase A = max.

The results of these scenarios are graphic dependences of the total APLs on the three-phase active power consumption. These graphic dependences for two types of conductors are shown in the following Figures 8–11. For the symmetrical state (scenario 1), the graphic dependence was the same, as shown in Figure 5 and in Figure 6.

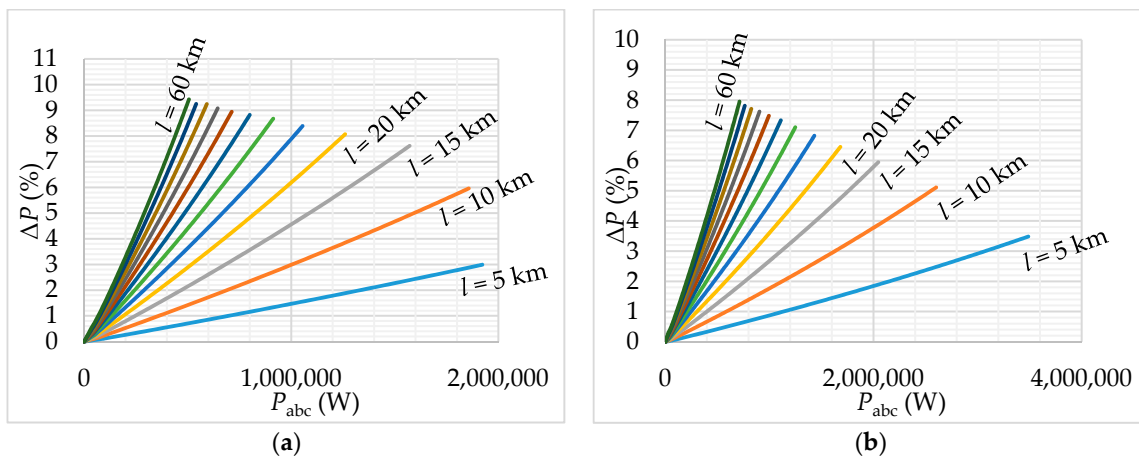


Figure 8. Scenario 2: (a) ACSR 42/7; (b) ACSR 70/11.

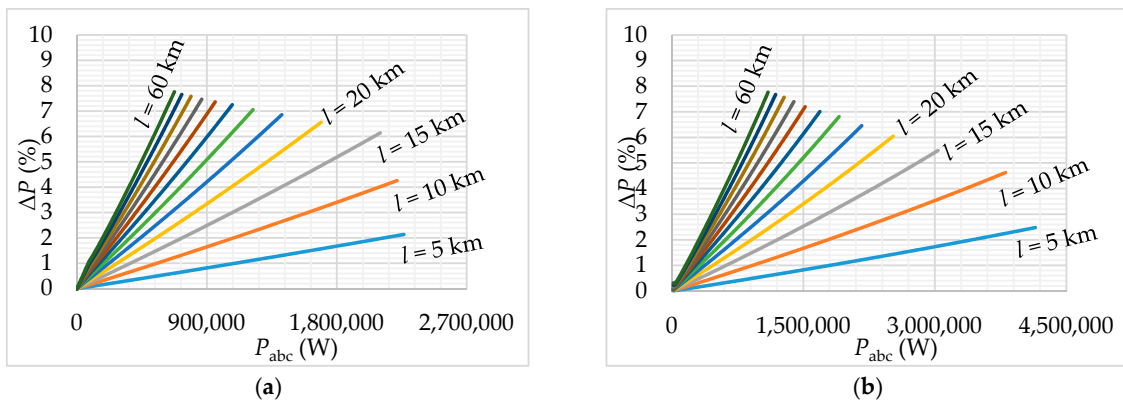


Figure 9. Scenario 3: (a) ACSR 42/7; (b) ACSR 70/11.

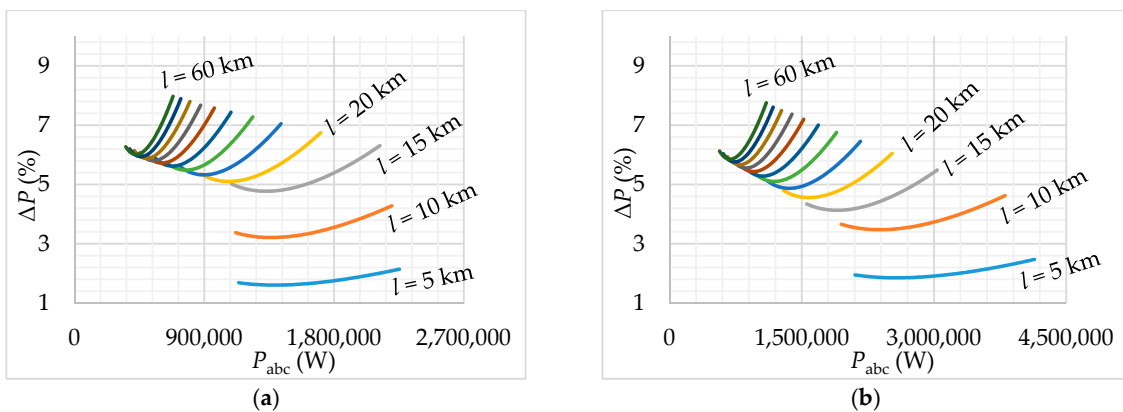


Figure 10. Scenario 4: (a) ACSR 42/7; (b) ACSR 70/11.

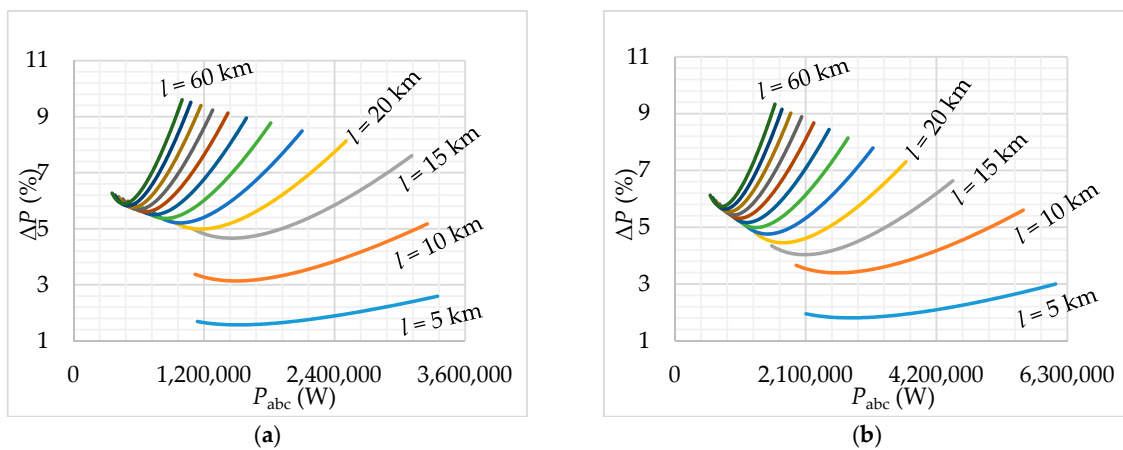


Figure 11. Scenario 5: (a) ACSR 42/7; (b) ACSR 70/11.

From these figures, it follows that the magnitude of APL depends not only on the three-phase active power consumption, the type, and the length of power line conductors, but also on the individual phases load. These figures also show how the load can be divided in each phase and how big the magnitudes of the current flowing are. We can say that if the length of the power line increases, the APLs will also increase. If the three-phase active power consumption increases, the APLs will also increase. If we compare these APLs caused by the load unbalance to the APLs for the symmetric state, the three-phase active power consumption decreased by the same size for the APLs. For example, the conductor ACSR 70/11 with a length of 5 km and APLs of 2%, the three-phase active power consumption was 2.15 MW (Figure 8b). The three-phase active power consumption was 4.27 MW for the symmetric state and the APLs of 2%.

The results of scenario 3 (Figure 9) were similar to the previous case. If we compare this scenario to scenario 2, the three-phase active power consumption was larger for the same APLs. It was caused by the uniform load in two phases.

Scenario 4 and scenario 5 were similar according to the results. These results are shown in Figures 10 and 11. The APLs decreased to certain values of the three-phase active power consumption. After the drop, the APLs started to rise. This change in the trend was caused by the increasing load during phase B, and the total load which was partially symmetric. Another reason was that the current of the neutral conductor in the LV side increased. The APL drop occurred until the current of the neutral conductor started to increase due to the increased load of phase B. The APLs started to increase again, and the three-phase active power consumption also increased.

4.3. The Influence of the Power Factor of the Fundamental Frequency on Active Power Losses

The increase of a reactive power, which flows in the grid was caused by worse PF. The overall grid current, which causes APLs, consists of the active component and the reactive component. Because of this, the reactive component of the current was minimized in this case. It results in the spreading of the active power mainly in the power line and the APL is at minimum.

The total APLs considering this PF can be defined as:

$$\begin{aligned} \Delta P_C &= \Delta P_1 + \Delta P_2 + \Delta P_3 = R_1 \cdot I_1^2 + R_2 \cdot I_2^2 + R_3 \cdot I_3^2 \\ &= R_1 \cdot \left(\frac{P_1^2}{V_1^2 \cdot \cos^2 \varphi_1} \right) + R_2 \cdot \left(\frac{P_2^2}{V_2^2 \cdot \cos^2 \varphi_2} \right) + R_3 \cdot \left(\frac{P_3^2}{V_3^2 \cdot \cos^2 \varphi_3} \right). \end{aligned} \quad (26)$$

From Formula (26), it follows that if the resistances of the individual power line phase R , the active powers P and phase-to-phase voltages V are constant, then the APLs are indirectly proportional to the square of the fundamental power frequency factor. The increase of the APLs caused by the change of PF are shown in Figures 12–14.

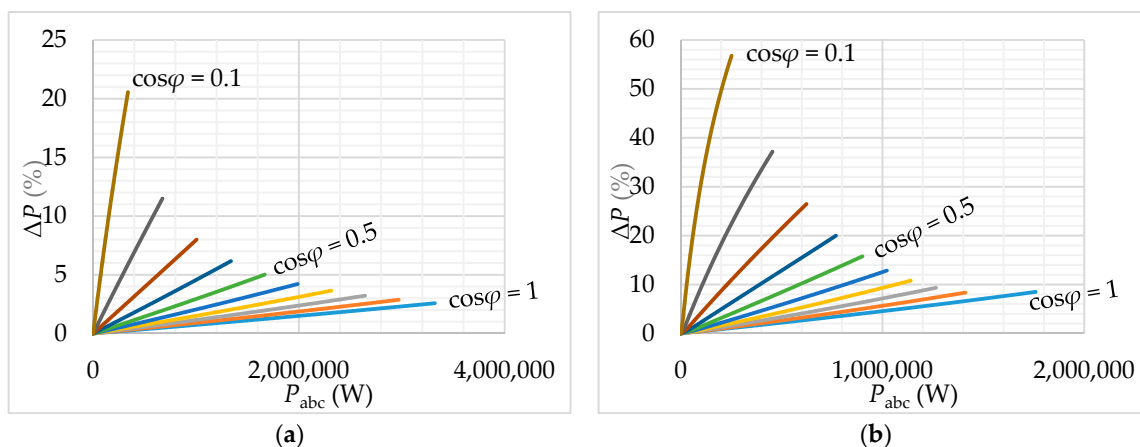


Figure 12. The dependence of increasing APLs from three-phase active power consumption for ACSR 42/7: (a) the length of 5 km; (b) the length of 30 km.

From these figures, it follows that:

- Three-phase active power consumption decreased due to the aggravate PF.
- The APLs in the power line increased due to the aggravate PF.
- Three-phase active power consumption decreased due to the aggravate PF and increased in the length of the power line.
- The APL in the power line increased due to the aggravate PF and increased in the length of the power line.

- If the cross-section of the power line conductor is increased, the three-phase active power is increased at the given PF.
- If the cross-section of the power line conductor is increased, the APLs are decreased at the given PF.

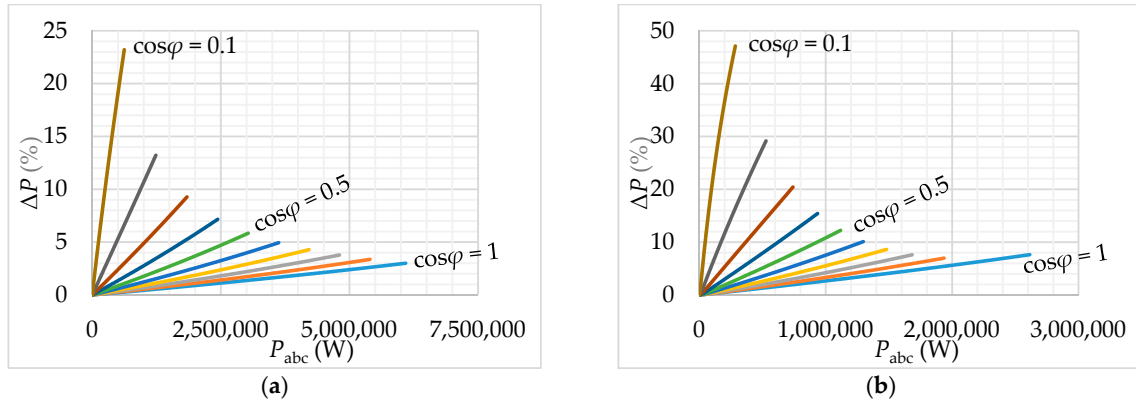


Figure 13. The dependence of increasing APLs from three-phase active power consumption for ACSR 70/11: (a) the length of 5 km; (b) the length of 30 km.

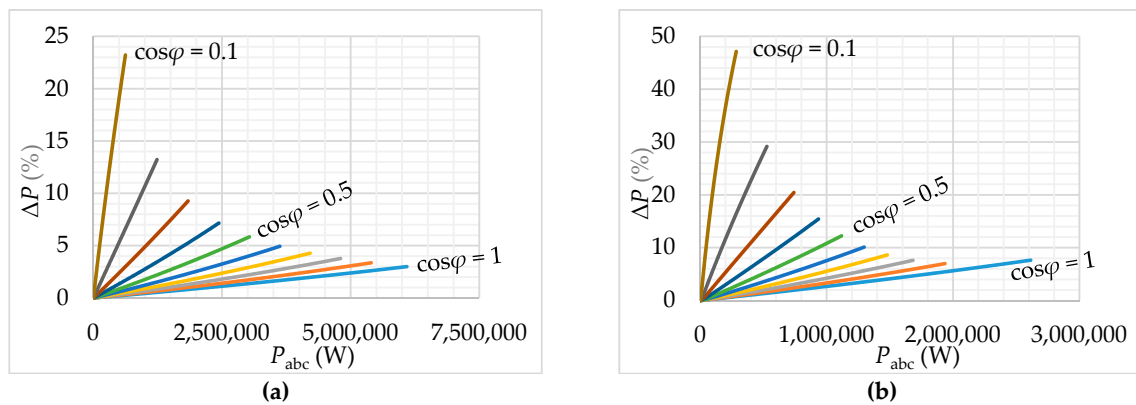


Figure 14. The dependence of increasing APLs from three-phase active power consumption for ACSR 95/15: (a) the length of 5 km; (b) the length of 30 km.

4.4. The Influence of Harmonics on Active Power Losses

The inharmonic grid current causes APLs, which correspond to the square of its RMS value. Active work only provides a real part of the fundamental harmonic current (in this case, if we have a non-linear appliance connected to the harmonic voltage source), currents of higher harmonic orders can be considered as the reactive component of the current of the fundamental harmonic. The increase of APLs in the grid can be determined as:

$$\frac{\Delta P_H}{\Delta P_1} = \frac{R \cdot I_H^2}{R \cdot I_1^2} = \frac{\sum_{h=1}^H I_h^2}{I_1^2} = \frac{I_1^2 + \sum_{h=2}^H I_h^2}{I_1^2} = 1 + THD_{I, STN EN 50160}^2 \quad (27)$$

The total APLs, which are caused by the higher harmonics can be calculated for a MV three-phase system as:

$$\begin{aligned} \Delta P_C &= \sum_{h=1}^{\infty} R_{1st_h} \cdot I_{1_h}^2 + \sum_{h=1}^{\infty} R_{2st_h} \cdot I_{2_h}^2 + \sum_{h=1}^{\infty} R_{3st_h} \cdot I_{3_h}^2 \\ &= R_{1st_1} \cdot I_{1_1}^2 + \sum_{h=2}^{\infty} R_{1st_h} \cdot I_{1_h}^2 + R_{2st_1} \cdot I_{2_1}^2 + \sum_{h=2}^{\infty} R_{2st_h} \cdot I_{2_h}^2 + R_{3st_1} \cdot I_{3_1}^2 + \sum_{h=2}^{\infty} R_{3st_h} \cdot I_{3_h}^2, \end{aligned} \quad (28)$$

where $R_{1st}, R_{2st}, R_{3st}$ are frequency dependent resistances of the individual conductors of h -harmonic; $R_{1st1}, R_{2st1}, R_{3st1}$ are frequency dependent resistances of the individual conductors of the fundamental harmonic; I_{1h}, I_{2h}, I_{3h} are currents of the individual conductors of h -harmonic; I_{11}, I_{21}, I_{31} are currents of the individual conductors of fundamental harmonics.

From Formula (28), it follows that the total APLs in the power line were created not only from the current of the first harmonic, but also from the current of the individual higher harmonics.

Harmonic line loss refers to the network loss caused by harmonics. Harmonic power has no other benefit than creating the heat, but it is consumed in the form of heat in all aspects of the transmission process and in electrical equipment. Therefore, harmonic power is essentially the line loss-harmonic caused by harmonics. Therefore, the positive harmonic power increases the line loss of the power system. In addition to the increase of line loss, harmonics will also cause a decrease in the power factor, which indirectly leads to an increase in power loss. Reducing the harmonic line loss is due to the energy conservation and emission reduction of power grid companies [42].

The increase of APL that are caused by the higher harmonics is shown in Figures 15–17. However, the higher harmonics does not create work, therefore the power flowing through the grid depends only on the fundamental harmonic. The value of current flowing through the power line and the APL increased by these higher harmonics are counted to the APL caused by the fundamental harmonic.

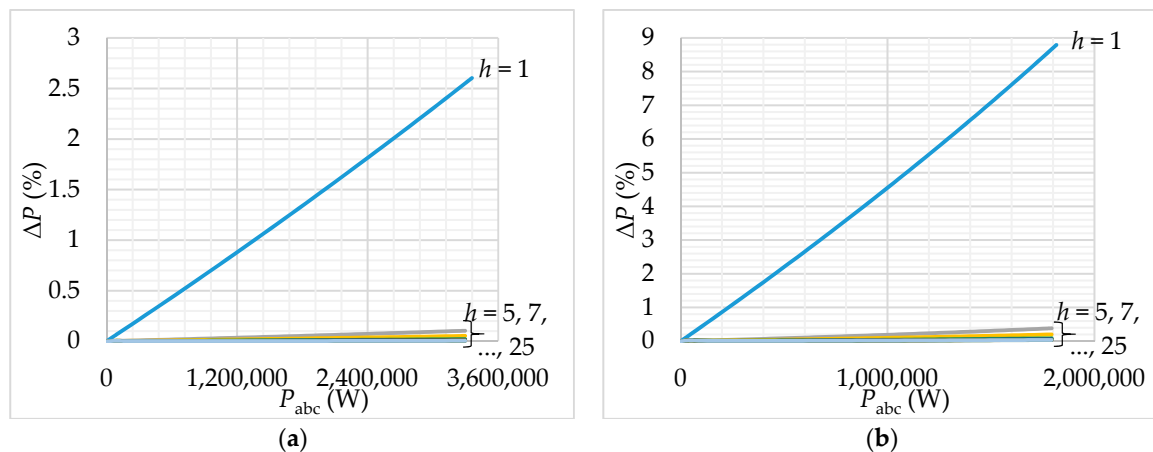


Figure 15. The dependence of increasing APLs from three-phase active power consumption for ACSR 42/7: (a) the length of 5 km; (b) the length of 30 km.

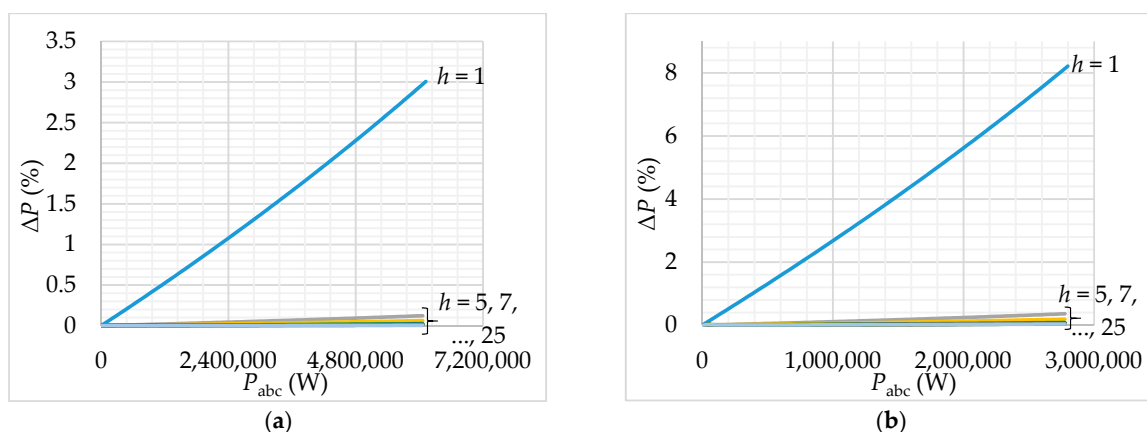


Figure 16. The dependence of increasing APLs from three-phase active power consumption for ACSR 70/11: (a) the length of 5 km; (b) the length of 30 km.

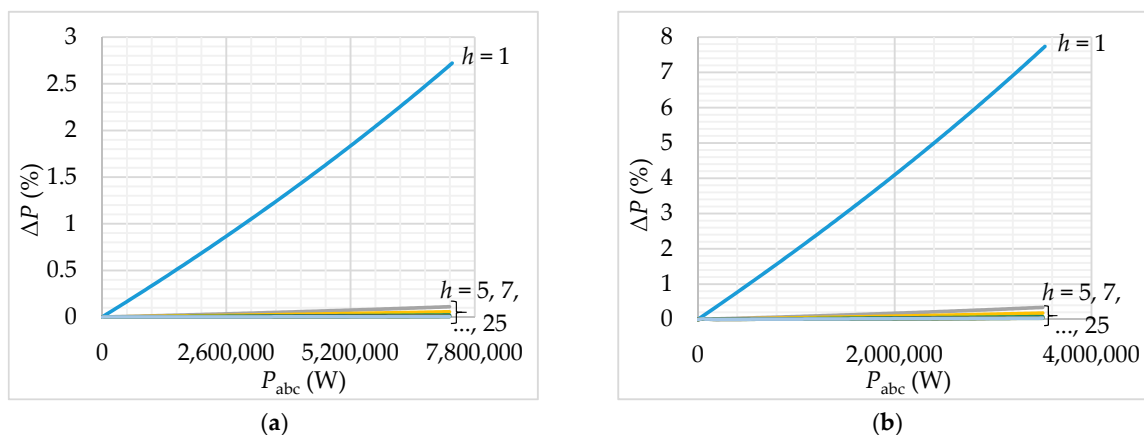


Figure 17. The dependence of increasing APLs from three-phase active power consumption for ACSR 95/15: (a) the length of 5 km; (b) the length of 30 km.

5. Measurement of the Influence of Certain Power Quality Parameters on the Technical Losses on the Physical Model of Distribution of a 22-kV Grid

In distribution grids, the limit values of qualitative parameters can be exceeded. The qualitative parameters must fulfill certain limits set by the standard STN EN 50 160. The AEs with the greatest impact on technical losses of electrical energy in distribution grids can be considered to be the PF, load unbalance, and the occurrence of higher current harmonics. This chapter is focused on the analysis of the influence of these three factors on the APLs, which were measured on the physical model of distribution on a 22-kV grid.

The model of 22-kV distribution grid is represented by RLC parameters and it was constructed at a 1:100 scale. The concept of the model was based on the combination of three basic single-phase π -sections of passive electrical elements. These π -sections were connected to a common electrical ground. They consisted of different modules with lengths of 2.5 km, 5 km, and 10 km using ACSR conductors. Conductors with lengths of 2.5 km and 5 km used ACSR 95/15, ACSR 70/11, and ACSR 42/7, and the one with a length of 10 km used ACSR 95/15 [43]. The measured scheme of this distribution grid is shown in Figure 18. This grid serves like a source of data for the next analysis of individual factors.

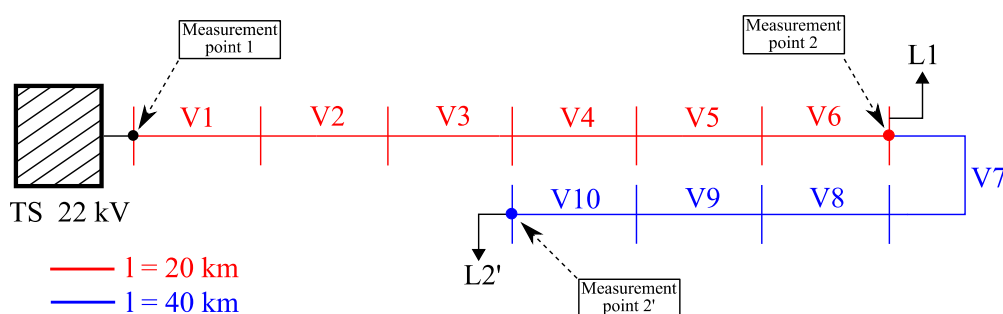


Figure 18. Distribution grid for the analysis of the influence of individual factors.

Power line sections with lengths of 20 km and 40 km were measured. The first measurement point was situated at the start of the power line and the second measurement point was at the end of the power line. The load was connected at the end of power line. The measurement was performed by the quality analyzers, BK-ELCOM ENA 330, that were installed to the all measurement points. Root mean square values of voltages and currents, the active power, the reactive power, and the apparent power were evaluated at each measurement point. The APLs of the electrical energy were evaluated based on these measured values.

5.1. Analysis of Power Factor of the Fundamental Frequency Influence on the Active Losses

The PF was analyzed for five values (1, 0.95, 0.9, 0.85, 0.8) of inductive character, for two lengths of power line (20 km and 40 km), for three types of conductors (ACSR 42/7, ACSR 70/11, and ACSR 95/15), and for three types of demand (600 kW, 1200 kW, and 1800 kW). For a demonstration, the PF for the demand of 1200 kW was chosen and its graphic dependencies are shown in Figure 19.

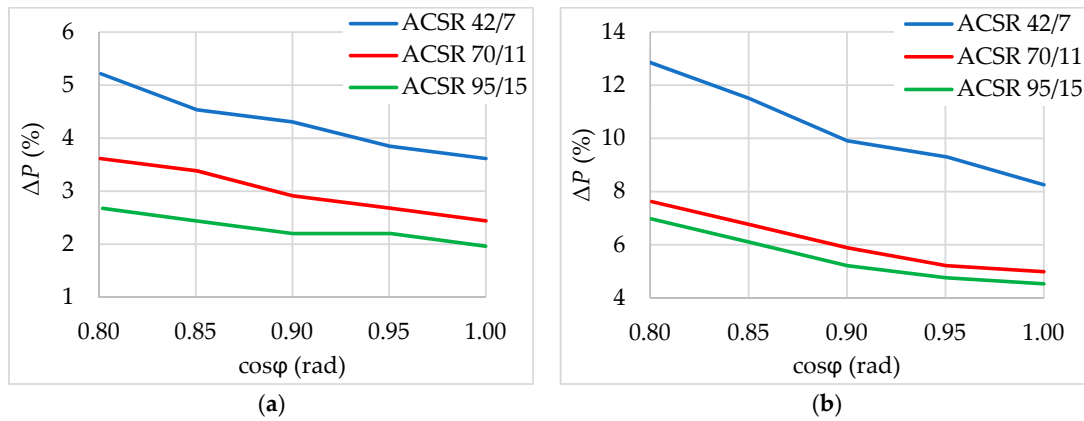


Figure 19. The graphic dependence of increasing APLs from power factor (PF): (a) the length of 20 km; (b) the length of 40 km.

We can see in Figure 19 that with the improving PF, the APLs drop due to the fact that the value of the reactive current component decreased, thus the total current flowing through the power line decreased.

The overall comparison of the APL caused by PF for the length of 20 km is shown in Figure 20. From Figure 20 it follows that the APLs increased due to the aggravated PF, because the reactive component of the current flowing through the power line increased. The total current increased due to this reason. If the cross-section of the power line conductor increased, the APL decreased. If the three-phase active power consumption increased, the APL increased, because the current flowing through the power line increased.

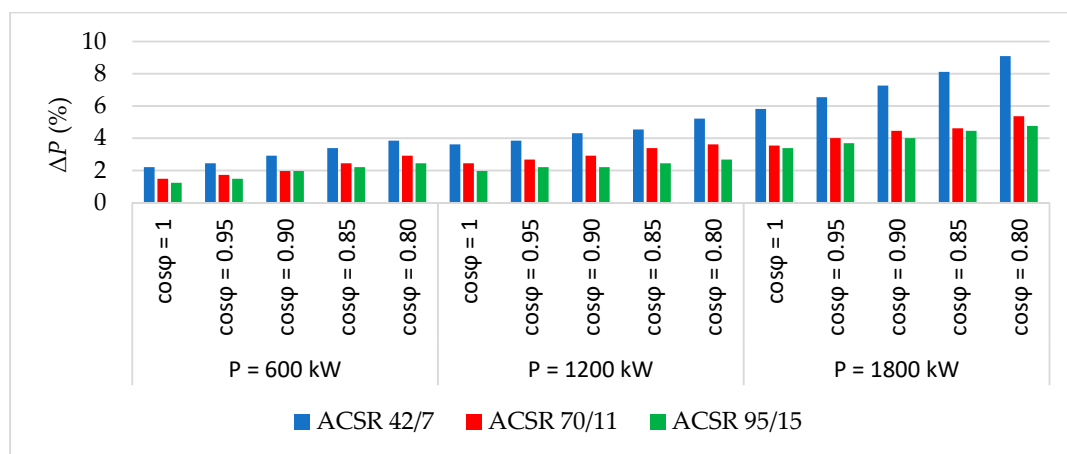


Figure 20. The comparison of the APLs for three types of active power and three types of conductors.

5.2. Analysis of the Influence of the Load Unbalance on the Active Power Losses

The analysis was performed with the load of constant power character. This active power was divided on the individual phases of power line in different percentage. For example, the active power consumption was 1200 kW. This power was divided in the individual phases in the ratio 40:40:20.

It means that the first phase was loaded by 480 kW, the second phase was 480 kW, and the third phase was 240 kW. For demonstration, the influence of power unbalance to the APL is shown in the following Figures 21–23 for the three types of conductors. We can see in these figures that the smallest APLs were for the conductor ACSR 95/15 due to its big cross-section and the smallest resistance in comparison with the other conductors. The biggest APLs were for the conductor ACSR 42/7. If the load unbalance between the individual phases of the power line was bigger, than the APLs were bigger. It was caused by the current flowing through the individual phases of the power line. From comparison of the ACSR conductors, it can be noted that sometimes the APLs can be decreased by more than a half by changing the conductor type.

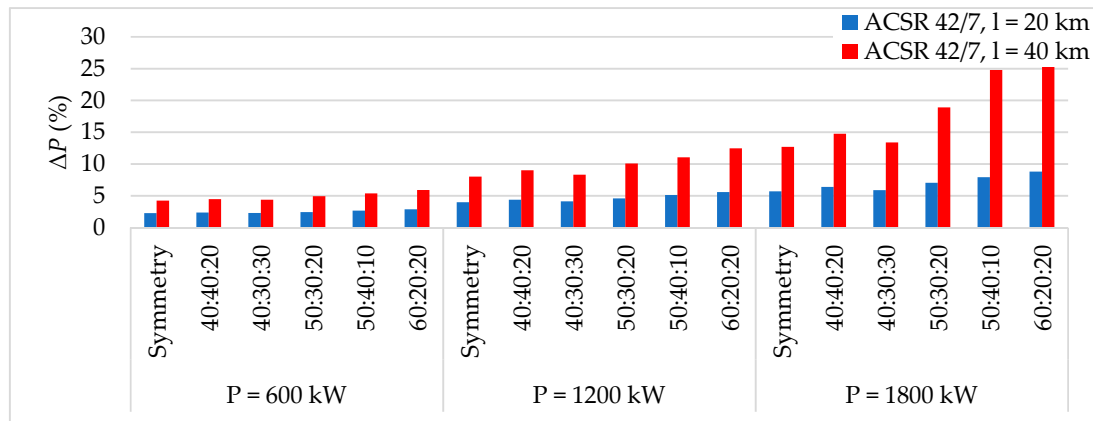


Figure 21. The comparison of the APLs for three types of active powers for conductor ACSR 42/7.

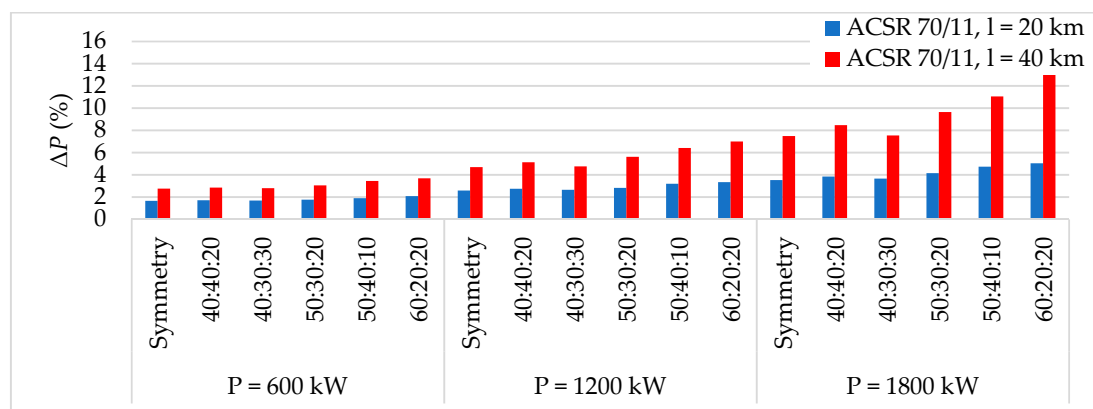


Figure 22. The comparison of the APLs for three types of active powers for conductor ACSR 70/11.

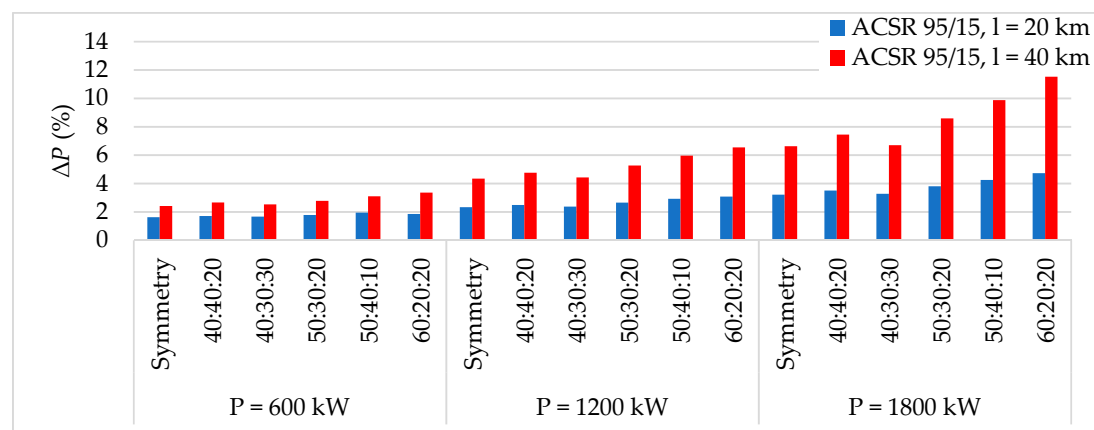


Figure 23. The comparison of the APLs for three types of active powers for conductor ACSR 95/15.

5.3. Analysis of the Influence of the Current Harmonics on the Active Losses

Current harmonics were caused by the three-phase full-wave rectifier with the bridge connection. Harmonics up to 15th order (considering the magnitude of current) have the biggest influence on distribution grids. The harmonics higher than ones of the 15th order only have a minimal influence on grids.

For the comparison of the APLs for the three active powers, two lengths of power line and three types of conductors are shown in Figures 24–26. It can be seen from these figures that non-harmonic currents flowing through the power line is growing with the APLs.

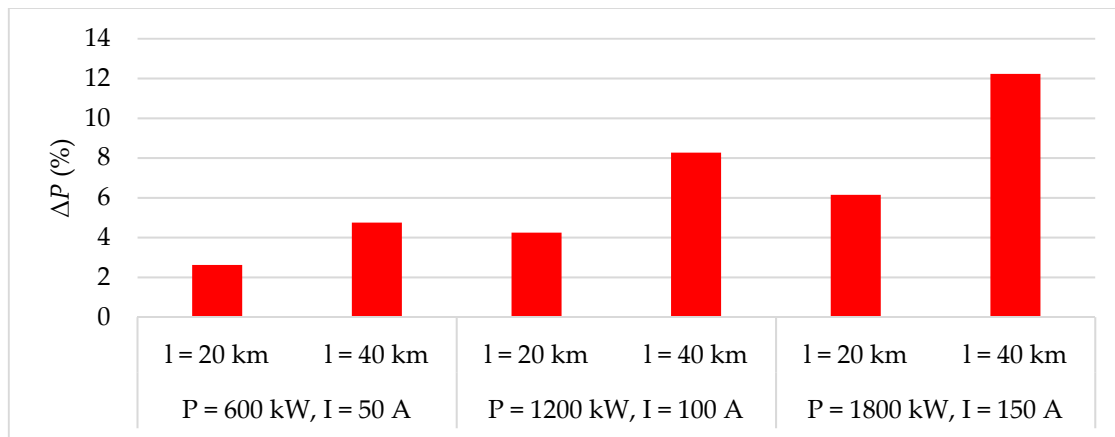


Figure 24. The comparison of the APLs for three types of active powers for conductor ACSR 42/7.

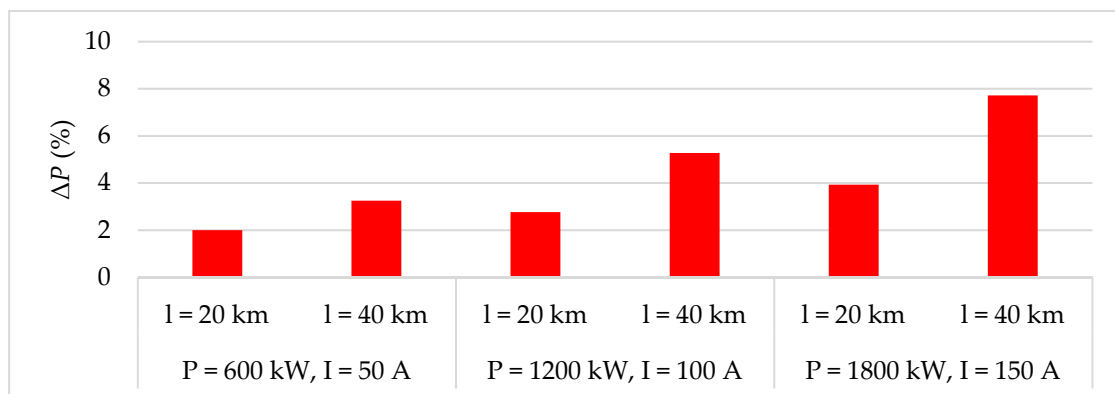


Figure 25. The comparison of the APLs for three types of active powers for conductor ACSR 70/11.

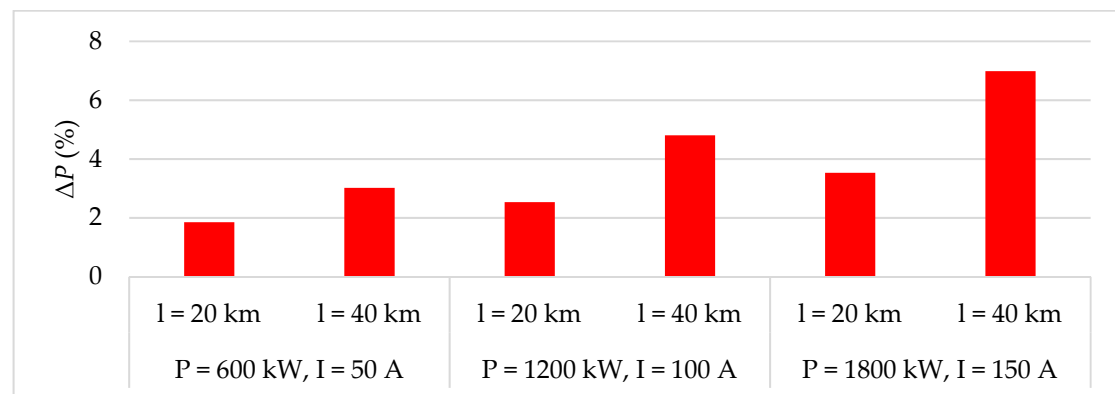


Figure 26. The comparison of the APLs for three types of active powers for conductor ACSR 95/15.

5.4. Comparison of the Measurement and Simulation

After analysis of the measurements of the individual factors affecting the size of the APLs, a simple grid (due to the availability of the power lines modules) was created using an existing physical model of a distribution grid. This proposed grid was measured, and its simulation model was created, which is shown in Figure 27. The comparison of the real measuring data with the simulation results were done for verification of the correctness all reached results. A distribution grid is a tree structure topology that has 11 nodes (10 power lines). The power lines consist of three types of ACSR conductors with different lengths. Loads were connected to the three nodes. The first load that represents the influence of unbalance was connected to node 9 (L1). The second load that represents the influence of the PF was connected to node 6 (L2), and the load that represents the influence of the higher current harmonics was connected to node 11 (L3).

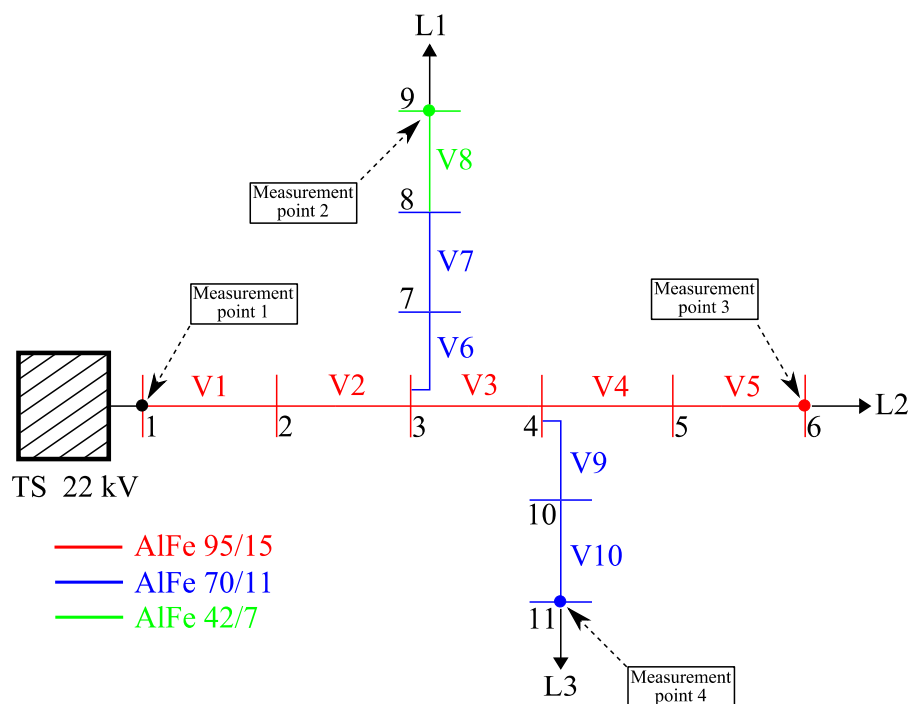


Figure 27. The scheme of measured and modelled distribution grid.

Real measurements were performed by the quality analyzer ENA 330 and were situated to the four nodes. The results of the measurement were compared with the results of simulation. The simulation model was created in the simulation program Matlab/Simulink.

The results of the measurement and simulation of the voltages and the currents at individual measurement points are shown in the following figures. It can be seen from the following figures that these graphic dependencies are approximately similar. It shows that the simulation was developed correctly. Firstly, Figure 28 represents the amplitude of voltages and currents of individual phases at the start of the power line.

The first load represents three-phase active power unbalance of 1200 kW. The power was divided with ratio 40:40:20 on individual phases, it represents the ratio of active power 480:480:240 kW. This ratio was chosen because this unbalance normally exists in the real distribution grid. The graphic dependencies are shown in Figure 29.

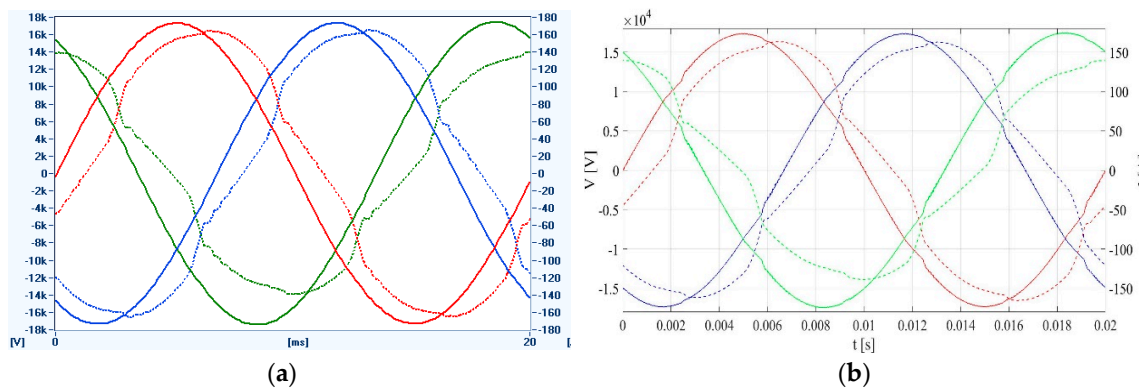


Figure 28. The voltages (full line) and the currents (chain line): (a) the measurement; (b) the simulation.

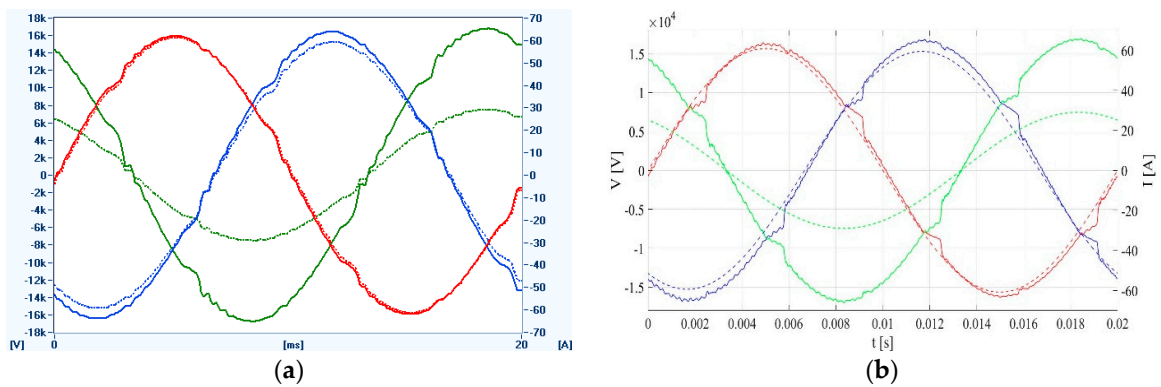


Figure 29. The voltages (full line) and the currents (chain line): (a) the measurement; (b) the simulation.

The second load was represented by an engine with the PF value of 0.77 with inductive character. The graphic dependencies are shown in Figure 30.

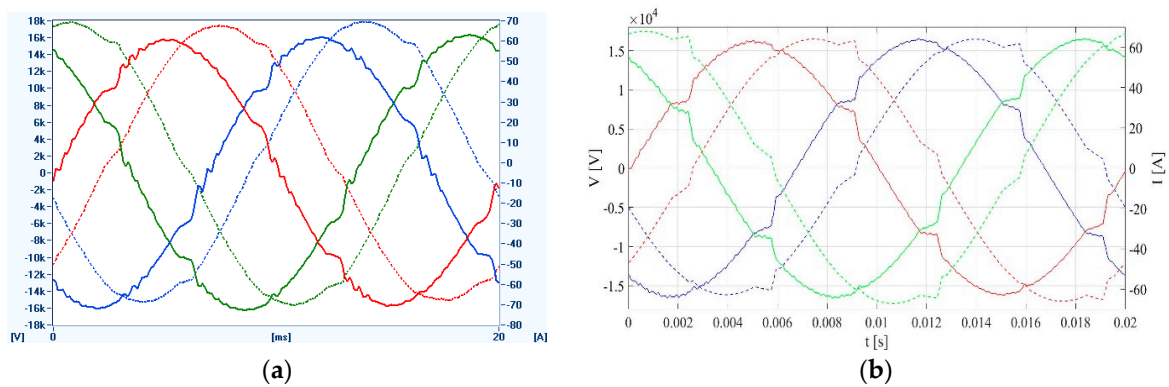


Figure 30. The voltages (full line) and the currents (chain line): (a) the measurement; (b) the simulation.

The third load represents the higher harmonics, which were spread to the distribution grid from the three-phase full-wave rectifier with bridge connection. The individual dependencies of currents and voltages are shown in Figure 31.

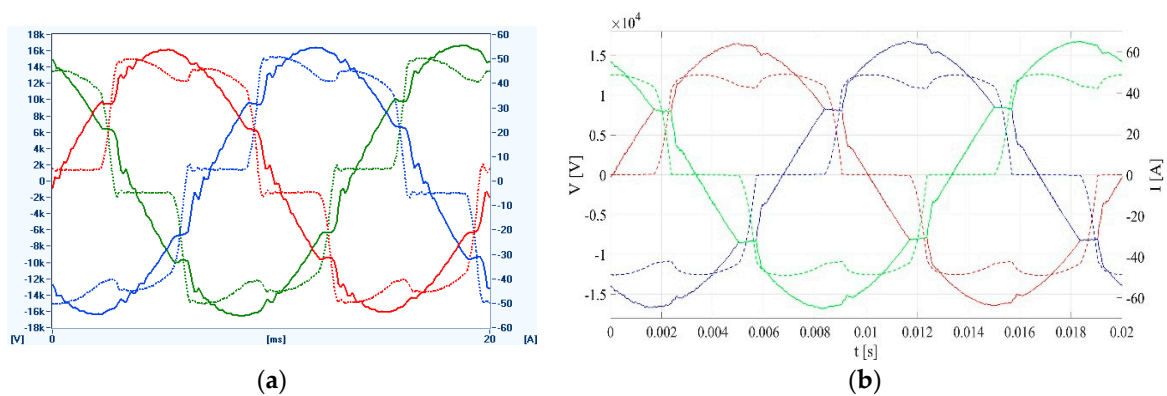


Figure 31. The voltages (full line) and the currents (chain line): (a) the measurement; (b) the simulation.

The voltages at individual measurement points in the distribution grid are shown in Figure 32. The values of the voltages were compared with the nominal phase voltage of the 22-kV distribution grid that was at a 12.7-kV voltage. Limited values, according to the standard STN EN 50160, were characterized for voltage swell or voltage dip in the individual phases, and are marked in Figure 32. The limit value of $\pm 10\% V_N$ in individual phases was exceeded during the measurement. This voltage dip could be caused, for example, by the imperfectly tuned power resistors of individual phases, transition resistance of terminals, coil resistances, or due to the parameters of individual modules or not considering the influence of heating in simulation, etc.

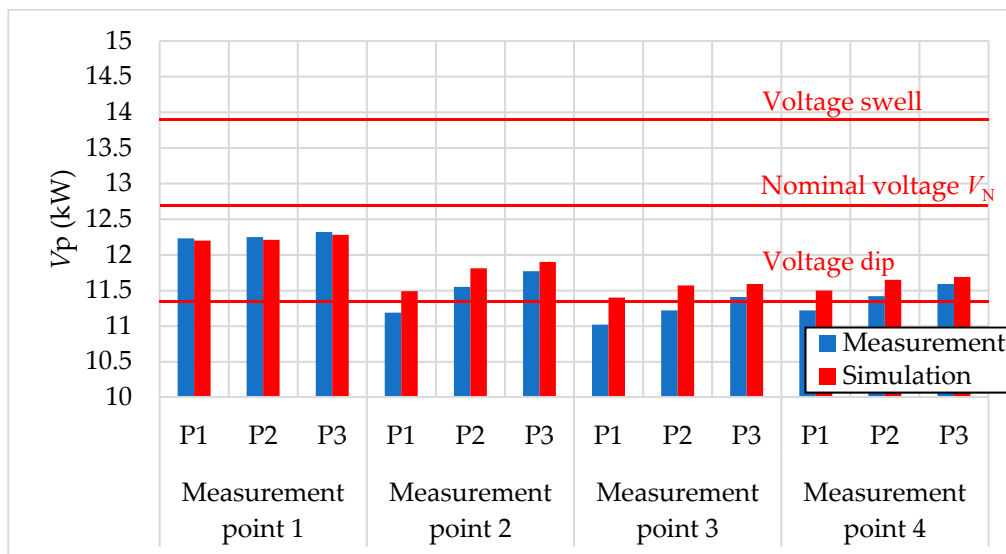


Figure 32. Voltage levels at the measurement points in the distribution grid.

The values of compared currents in individual phases from the measurement and the simulation results are shown in Figure 33 and the values of active power are shown in Figure 34.

Three-phase active power at the start of the power line and at the end of the power line are shown in Table 4. The APLs that were obtained by the simulation and the measurement were approximately similar with the value of 5%, representing an active power of 190 kW. We can say that the results of the measurement and the results of the simulation are correct.

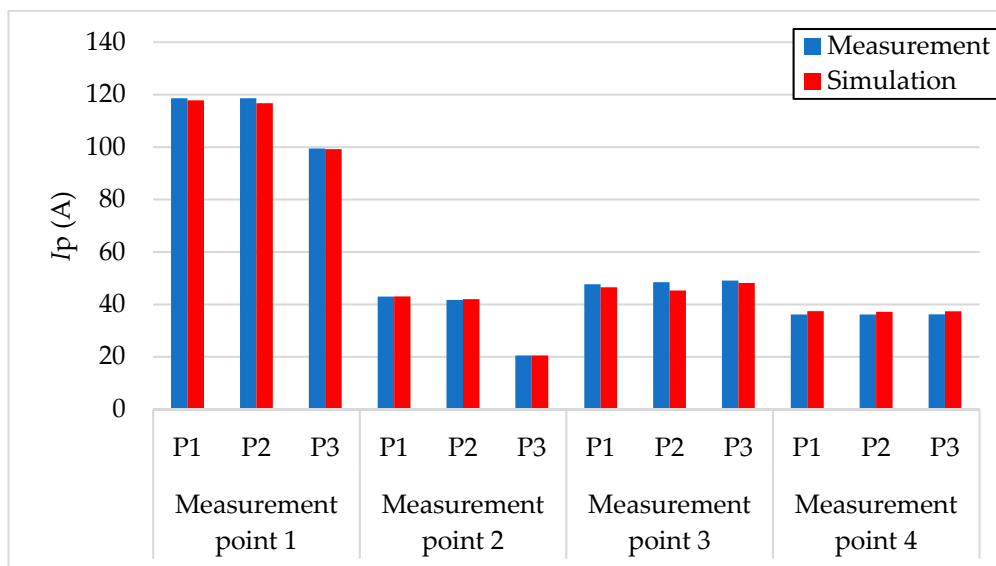


Figure 33. Current levels at the measurement points in the distribution grid.

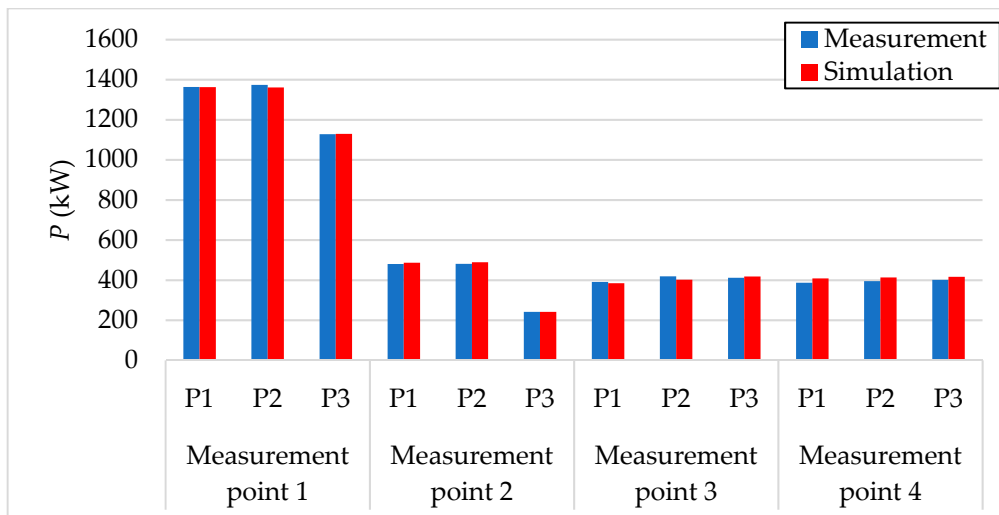


Figure 34. Active power levels at the measurement points in the distribution grid.

Table 4. Three-phase values of active power and active power losses.

Comparison	P_{ABC} (kW)	P_{abc} (kW)	ΔP (kW)	ΔP (%)
Measurement	3866.00	3662.70	203.30	5.259
Simulation	3854.90	3660.39	194.51	5.046

Total harmonic distortion of voltage THD_V , total harmonic distortion of current THD_I , and harmonic spectrum were evaluated at each measurement point. Figures 35 and 36 show the values of THD_I and THD_V in nodes of the distribution grid obtained from the simulation. It can be seen that the limit value of $THD_V < 8\%$, according to the standard STN EN 50160, was not exceeded at any measurement point. The maximal values of THD_V were in the nodes, where the individual non-linear loads were connected. The minimal values of THD_V were in the node at the start of the power line. The smallest values of THD_V were at the start of the power system, because the generation of voltage harmonics fell down in the direction to the upstream stiff system.

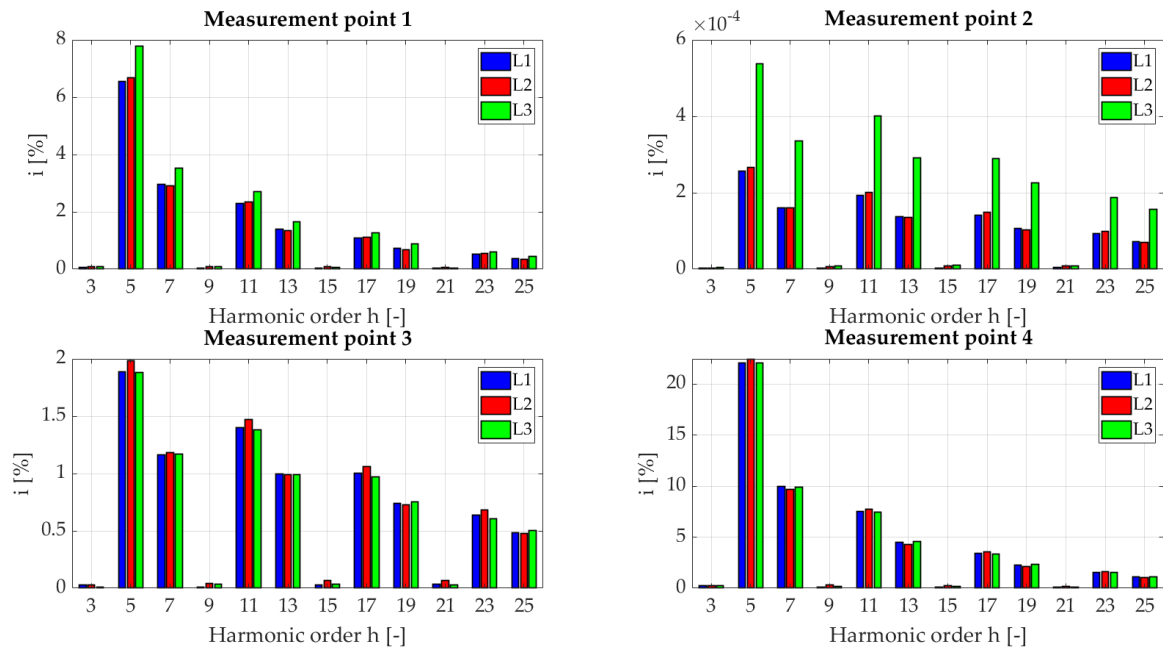


Figure 35. Current harmonic spectrum at the measurement points.

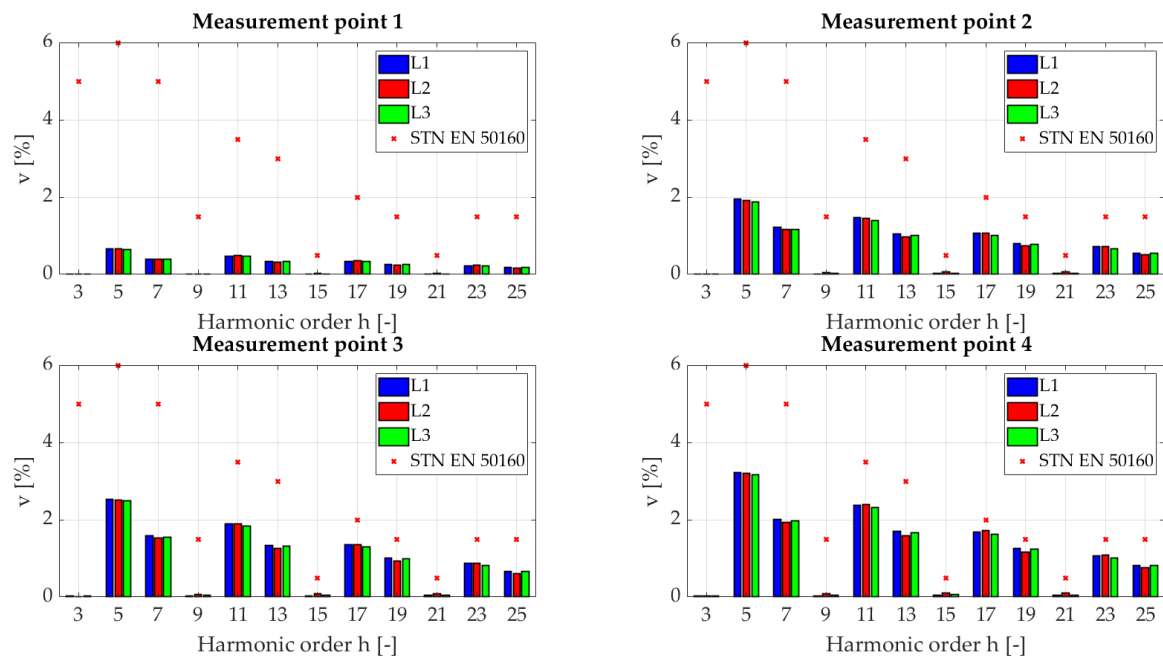


Figure 36. Voltage harmonic spectrum at the measurement points.

6. Results of Adverse Effects during the Certain Period

This chapter is focused on an indicative overview of the price growth for a distribution system operator over a certain period of time due to increased APLs in the distribution grid. This price growth was caused by the AEs. For demonstration, the APLs and financial losses per year for the conductor ACSR 70/11 are shown in Tables 5 and 6 for the length of 20 km and 40 km, respectively. Three-phase active power consumption was 1200 kW and price of power energy was 40 €/MW/h. The percentual APLs represent ΔP . Their size was calculated by the active power at the start of power line minus the active power at the end of power line. This difference was divided by the active power at the start of the power line and multiplied by 100%. This ΔP was multiplied by the load and we obtained the APL per hour. When the APLs per hour were multiplied by 24 (hours per day) and 365 (days per year),

we got the APLs per year. Additional losses ΔP_{ADD} were determined by the difference between the active power losses per year for the given APL and the active power losses per year for the symmetric state. This difference was multiplied by 40 Euros and we got the financial losses.

The most significant financial losses were caused by the load unbalance and the PF in the most extreme cases. The harmonics did not have a large impact on financial losses. Financial losses were more expressive for the length of 40 km than 20 km, because APLs were larger in the grids with greater length. In some of the cases, the price was triple in comparison with the price for the length of 20 km. Of course, the APLs varied depending on the conductor of the power line. The greatest APL and financial losses were for the conductor ACSR 42/7, and on the other side, the smallest were for the conductor ACSR 95/15.

Table 5. Overview of active power losses and their impact on finance (ACSR 70/11, length of 20 km).

Scenario	Load (kW)	Active Power Losses in MV Grid				Informative Price of Power Energy 40.00 EURO
		ΔP (%)	ΔP (MW per hour)	ΔP (MW per year)	ΔP_{Add} (MW per year)	
Symmetric	1233.7	2.586	0.0319	279.444	0	0.00 EURO
Unbalance 40:40:20	1235.3	2.752	0.0340	297.840	18.396	735.84 EURO
Unbalance 40:30:30	1233.8	2.650	0.0327	286.452	7.008	280.32 EURO
Unbalance 50:30:20	1236.3	2.831	0.0350	306.600	27.156	1086.24 EURO
Unbalance 50:40:10	1240.4	3.193	0.0396	346.896	67.452	2698.08 EURO
Unbalance 60:20:20	1242.5	3.348	0.0416	364.416	84.972	3398.88 EURO
cos ϕ = 0.8	1245.0	3.614	0.0450	394.200	114.756	4590.24 EURO
cos ϕ = 0.85	1242.0	3.382	0.0420	367.920	88.476	3539.04 EURO
cos ϕ = 0.9	1236.0	2.913	0.0360	315.360	35.916	1436.64 EURO
cos ϕ = 0.95	1233.0	2.676	0.0330	289.080	9.636	385.44 EURO
Harmonics	1204.4	2.765	0.0333	291.708	12.264	490.56 EURO

Table 6. Overview of active power losses and their impact on finance (ACSR 70/11, length of 40 km).

Scenario	Load (kW)	Active Power Losses in MV Grid				Informative Price of Power Energy ΔP (MW per hour)
		ΔP (%)	ΔP (MW per hour)	ΔP (MW per year)	ΔP (%)	
Symmetric	1261.0	4.687	0.0591	517.716	0	0.00 EURO
Unbalance 40:40:20	1265.4	5.129	0.0649	568.524	50.808	2032.32 EURO
Unbalance 40:30:30	1261.4	4.765	0.0601	526.476	8.760	350.40 EURO
Unbalance 50:30:20	1273.0	5.625	0.0716	627.216	109.500	4380.00 EURO
Unbalance 50:40:10	1283.9	6.410	0.0823	720.948	203.232	8129.28 EURO
Unbalance 60:20:20	1289.1	6.997	0.0902	790.152	272.436	10,897.44 EURO
cos ϕ = 0.8	1299.0	7.621	0.0990	867.240	349.524	13,980.96 EURO
cos ϕ = 0.85	1287.0	6.760	0.0870	762.120	244.404	9776.16 EURO
cos ϕ = 0.9	1275.0	5.882	0.0750	657.000	139.284	5571.36 EURO
cos ϕ = 0.95	1266.0	5.231	0.0660	578.160	60.444	2417.76 EURO
Harmonics	1211.4	5.275	0.0639	559.764	42.048	1681.92 EURO

7. Conclusions

This paper deals with the determination of APLs in a 22-kV distribution grid caused by AEs. The AEs studied in this paper were PF, load unbalance, and higher current harmonics. Based on comprehensive laboratory tests on AEs, the electric parameters were measured via a physical model of a 22-kV distribution grid. Basic APLs occur in every distribution or transmission system and they mainly depend on grid topology, the parameters of transformers, and the magnitude of the current flowing through the grid. These basic APLs are always determined for a symmetric state and they are increased by each of the abovementioned AEs.

For the worst AEs, PFs with a value less than 0.9 of inductive character and load unbalance can be considered. Higher harmonics did not cause significant financial losses. Every adverse effect can be reduced:

- by evenly distributed loads, which also influences the load unbalance,
- compensation devices, which also influences PF,
- passive and active filters, which also influences higher harmonic orders,
- active filters for each AE.

All of these AEs cause an increase in basic APLs. Although, the basic APLs increased about 0.1% in the distribution grid, and they can represent a big PL and financial losses for a distribution system operator during a certain period of time. This is why it is necessary to pay sufficient attention to losses and to find appropriate options for reducing, for example, those three investigated adverse effects on the distribution grid. It is always necessary to ask the question whether it is effective to reduce or minimize the given adverse effect also from the financial point of view—investment and return. It is difficult to say which option of reducing AEs would be the most effective and with a short period of financial return. Every investment in devices for reducing AE needs to be properly considered based on the measurement results.

Author Contributions: J.A. conducted a comprehensive overview of problematic electrical power networks and electrical power losses. A.O. conducted a comprehensive overview of problematic electrical power systems' quality and power lines. A.B., A.O., and J.A. created programs in Matlab for calculating power losses in distribution grids of 22 kV. A.B. and M.R. performed the measurements on the physical model of the distribution grid and wrote the paper.

Funding: This research received no external funding

Acknowledgments: This work was supported by the Slovak Research and Development Agency under the contract No. APVV-15-0464.

Conflicts of Interest: The authors declare no conflict of interest.

Abbreviations and Symbols

AE	Adverse effects
PQ	Power quality
PL	Power losses
LV	Low voltage
MV	Medium voltage
HV	High voltage
PF	Power factor of the fundamental frequency of electrical energy consumption
THD	Total harmonic distortion
HCV	Harmonic voltage
IHCV	Interharmonic voltage
BL	Basic losses
APL	Active power losses
RPL	Reactive power losses
ACSR	Aluminium conductor, steel reinforced
P	Active power (W)
Q	Reactive power (var)
S	Apparent power (VA)
V	Voltage (V)
I	Current (A)
R	Resistance of the power line (Ω)
X_L	Inductive reactance of power line (Ω)

References

1. Momoh, J.A. *Electric Power System Applications of Optimization*, 2nd ed.; CRC Press: Boca Raton, FL, USA, 2008; pp. 1–3.
2. Sayed Ishtiaque, A.M.; Islam, T.; Azad, H.M.; Kaiser Hamid Rocky, A.H.M. Optimization of the electrical power consumption for the domestic consumers using cutting-edge technology. *Int. J. Sci. Eng. Res.* **2014**, *5*, 296–301.
3. Ceaki, O.; Seritan, G.; Vatu, R.; Mancasi, M. Analysis of power quality improvement in smart grids. In Proceedings of the 10th International Symposium on Advanced Topics in Electrical Engineering ATEE 2017, Bucharest, Romania, 23–25 March 2017.
4. Suslov, K.V.; Solonina, N.N.; Smirnov, A.S. Distributed power quality monitoring. In Proceedings of the 16th International Conference on Harmonics and Quality of Power ICHQP 2014, Bucharest, Romania, 25–28 May 2014.
5. Tinoco De Rubira, T.A. Numerical Optimization and Modeling Techniques for Power System Operations and Planning. Ph.D. Thesis, Stanford University, Stanford, CA, USA, 2015.
6. Zobaa, A.F.; Canteli, M.M.; Bansal, R. *Power Quality Monitoring, Analysis and Enhancement*, 1st ed.; InTech: Rijeka, Croatia, 2011.
7. Dugan, R.C.; McGranaghan, M.F.; Santoso, S.; Wayne Beaty, H. *Electrical Power System Quality*, 3rd ed.; McGraw-Hill Education: New York, NY, USA, 2012.
8. Vinayagam, A.; Swarna, K.S.V.; Khoo, S.Y.; Stojcevski, A. Power quality analysis in microgrid: An experimental approach. *J. Power Energy Eng.* **2016**, *4*, 17–34. [[CrossRef](#)]
9. Singh, B.; Chandra, K.; Al-Haddad, K. *Power Quality Problems and Mitigation Techniques*, 1st ed.; John Wiley and Sons Ltd.: Chichester, UK, 2015.
10. Belany, P.; Bolf, A.; Novak, M.; Roch, M. The impact of small non-linear load operation on accuracy of the intelligent measurement system. In Proceedings of the International Conference and Expositions on Electrical and Power Engineering EPE 2018, Iasi, Romania, 18–19 October 2018.
11. Zobaa, A.F. *Power Quality Issues*, 1st ed.; InTech: Rijeka, Croatia, 2013.
12. Kus, V.; Bilik, P. Effects of small non-linear loads on the power grid. In Proceedings of the 9th International Scientific Symposium on Electrical Power Engineering, Stara Lesna, Slovakia, 12–14 September 2017; Technical University of Kosice: Kosice, Slovakia, 2017.
13. Suslov, K.; Solonina, N.; Gerasimov, D. Assessment of an impact of power supply participants on power quality. In Proceedings of the 18th International Conference on Harmonics and Quality of Power ISHQP 2018, Ljubljana, Slovenia, 13–16 May 2018.
14. Yadaiah, C.; Goswami, S.K.; Debashis, C. Effect of network reconfiguration on power quality of distribution system. *Int. J. Electr. Power Energy Syst.* **2016**, *83*, 87–95.
15. Bolf, A.; Otcenasova, A.; Roch, M.; Regula, M.; Belany, P. Influence of housing developments on voltage quality in distribution point. In Proceedings of the 12th International Conference ELEKTRO 2018, Mikulov, Czech Republic, 21–23 May 2018.
16. Montoya, F.G.; Banos, R.; Alcayde, A.; Montoya, M.G.; Manzano-Agugliaro, F. Power quality: Scientific collaboration networks and research trends. *Energies* **2018**, *11*, 2067. [[CrossRef](#)]
17. Jmail, U.; Amin, A.; Mahmood, A. A comparative study of control techniques for power loss minimization in a distribution network. In Proceedings of the 1st International Conference on Power, Energy and Smart Grid ICPEGS 2018, Mirpur Azad Kashmir, Pakistan, 9–10 April 2018.
18. Bhatti, S.S.; Lodhi, M.U.U.; Haq, S.; Gardezi, S.N.M.; Javaid, M.A.; Raza, M.Z.; Lodhi, M.I.U. Electric power transmission and distribution losses overview and minimization in Pakistan. *Int. J. Sci. Eng. Res.* **2015**, *6*, 1108–1112.
19. Au, M.T.; Anthony, T.M.; Kamaruddin, N.; Verayiah, R.; Syed Mustaffa, S.A.; Yusoff, M. A simplified approach in estimating technical losses in distribution network based on load profile and feeder characteristics. In Proceedings of the 2nd International Power and Energy Conference, Johor Bahru, Malaysia, 1–3 December 2008.
20. European Commission. Press Release Database, 2030 Climate and Energy Goals for a Competitive, Secure and Low-Carbon EU Economy. 2018. Available online: http://europa.eu/rapid/press-release_IP-14-54_en.htm (accessed on 19 February 2018).

21. Tuzikova, V.; Tlustý, J.; Müller, Z. A novel power losses reduction method based on a particle swarm optimization algorithm using STATCOM. *Energies* **2018**, *11*, 2851. [[CrossRef](#)]
22. Tran, Q.T.T.; Di Silvestre, M.L.; Sanseverino, E.R.; Zizzo, G.; Pham, T.N. Driven primary regulation for minimum power losses operation in islanded microgrids. *Energies* **2018**, *11*, 2890. [[CrossRef](#)]
23. El-salam, M.F.A.; Beshr, E.; Eteiba, M.B. A new hybrid technique for minimizing power losses in a distribution system by optimal sizing and siting of distributed generators with network reconfiguration. *Energies* **2018**, *11*, 3351. [[CrossRef](#)]
24. Truong, A.V.; Ton, T.N.; Nguyen, T.T.; Duong, T.L. Two states for optimal position and capacity of distributed generators considering network reconfiguration for power loss minimization based on runner root algorithm. *Energies* **2019**, *12*, 106. [[CrossRef](#)]
25. Arias, J.; Calle, M.; Turizo, D.; Guerrero, J.; Candelo-Becerra, J.E. Historical load balance in distribution systems using the branch and bound algorithm. *Energies* **2019**, *12*, 1219. [[CrossRef](#)]
26. Zhong-zheng, T.; Yang-zi, S. Study on unbalanced power flow in distribution network with distributed generators of power grid. In Proceedings of the China International Conference on Electricity Distribution CIGRE 2016, Xi'an, China, 10–13 August 2016.
27. STN EN 50160. *Voltage Characteristics of Electricity Supplied by Public Electricity Networks*; The Slovak version of the European Standard EN 50160; Slovak Office of Standards, Metrology and Testing: Bratislava, Slovak Republic, 2015.
28. *IEEE Guide for Application of Power Electronics for Power Quality Improvement on Distribution Systems Rated 1 kV Through 38 kV*; IEEE Std 1409-2012; IEEE: Piscataway, NJ, USA, 2012; pp. 1–90.
29. Tellez, A.A.; Lopez, G.; Isaac, I.; Gonzalez, J.W. Optimal reactive power compensation in electrical distribution systems with distributed resources. *Rev. Heliyon* **2018**, *4*, 1–30.
30. Gatta, F.M.; Geri, A.; Maccioni, M.; Mantineo, A.; Cresta, M.; Paulucci, M. Reactive power control strategy for voltage regulation and power-factor correction in MV distribution networks. In Proceedings of the IEEE Eindhoven PoweTech, Eindhoven, The Netherlands, 29 June–2 July 2015.
31. Bolf, A.; Otcenasova, A.; Regula, M.; Novak, M. Superposition of current and voltage harmonics. In Proceedings of the 12th International Conference ELEKTRO 2018, Mikulov, Czech Republic, 21–23 May 2018.
32. Chen, B.; Xiang, K.; Yang, L.; Su, Q.; Huang, D.; Huang, T. Theoretical line loss calculation of distribution network based on the integrated electricity and line loss management system. In Proceedings of the China International Conference on Electricity Distribution CIGRE 2018, Tianjin, China, 17–19 September 2018.
33. Feng, S.; Licheng, Y.; Zhitong, G.; Yanhong, C. Reactive power optimization compensation of line losses calculation in rural areas. In Proceedings of the Chinese Control and Decision Conference CCDC 2018, Shenyang, China, 9–11 June 2018.
34. Al-Mahroqi, Y.; Metwally, I.A.; Al-Hinai, A.; Al-Badi, A. Reduction of power losses in distribution systems. *Int. J. Comput. Syst. Eng.* **2012**, *6*, 315–322.
35. Mahmood, M.; Shivam, O.; Kumar, P.; Krishnan, G. Real time study on technical losses in distribution system. *Int. J. Adv. Res. Electr. Electron. Instrum. Eng.* **2014**, *3*, 131–137.
36. Kundu, M.; Jadhav, S.; Bagdia, K. Technical loss reduction through active repair of distribution transformer: Results from the field. In Proceedings of the 7th International Conference on Power Systems ICPS 2017, Pune, India, 21–23 December 2017.
37. Navani, J.P.; Sharma, N.K.; Sapra, S. Technical and non-technical losses in power system and its economic consequence in Indian economy. *Int. J. Electron. Comput. Sci. Eng.* **2003**, *1*, 757–761.
38. Chauhan, A.; Rajvanshi, S. Non-technical losses in power system: A review. In Proceedings of the International Conference on Power, Energy and Control, Sri Ranganalathum ICPEC 2013, Dindigul, India, 6–8 February 2013.
39. Electricity Distribution Systems Losses Non-Technical Overview. 2009. Available online: <https://www.ofgem.gov.uk/sites/default/files/docs/2009/05/sohn-overview-of-losses-final-internet-version.pdf> (accessed on 10 February 2019).
40. Ganesh, V.; Kumar, I. Power loss reduction distribution system by placing optimal capacitor banks. *Int. J. Adv. Res. Electr. Electron. Instrum. Eng.* **2016**, *5*, 713–721.
41. Tellez, A.A.; Galarza, D.F.C.; Matos, L.O. Analysis of power losses in the asymmetric construction of electric distribution systems. *IEEE Lat. Am. Trans.* **2015**, *13*, 2190–2194. [[CrossRef](#)]

42. Wang, Y.; Li, Y.; Liu, Z.; Jin, J.; Liu, X.; Yang, Y. Harmonic line loss suppression and rectification measures. In Proceedings of the China International Conference on Electricity Distribution, Tianjin, China, 17–19 September 2018.
43. Bolf, A.; Otcenasova, A.; Belany, P.; Susko, F. Synchronization device for the model of distribution grid 22 kV. In Proceedings of the 2017 6th International Youth Conference on Energy, Budapest, Hungary, 21–24 June 2017.



© 2019 by the authors. Licensee MDPI, Basel, Switzerland. This article is an open access article distributed under the terms and conditions of the Creative Commons Attribution (CC BY) license (<http://creativecommons.org/licenses/by/4.0/>).